# Magmatic evolution of the Nevado del Ruiz volcano, Central Cordillera, Colombia
## Mineral chemistry and geochemistry

N. VATIN-PÉRIGNON [1], P. GOEMANS [1], R.A. OLIVER [2]
L. BRIQUEU [3], J.C. THOURET [4], R. SALINAS E. [5], A. MURCIA L. [6]

**Abstract :** The Nevado del Ruiz, located 120 km west of Bogotá, is one of the currently active andesitic volcanoes that lies north of the Central Cordillera of Colombia at the intersection of two dominant fault systems originating in the Palaeozoic basement.

The pre-volcanic basement is formed by Palaeozoic gneisses intruded by pre-Cretaceous and Tertiary granitic batholiths. They are covered by lavas and volcaniclastic rocks from an eroded volcanic chain dissected during the late Pliocene.

The geologic history of the Nevado del Ruiz records two periods of building of the compound volcano. The stratigraphic relations and the K-Ar dating indicate that effusive and explosive volcanism began approximately 1 Ma ago with eruption of differentiated andesitic lava and pyroclastic flows and andesitic domes along a regional structural trend. Cataclysmic eruptions opened the second phase of activity. The upper sequences consist of block-lavas and lava domes ranging from two pyroxene-andesites to rhyodacites. Holocene to recent volcanic eruptions, controlled by the intense tectonic activity at the intersection of the Palestina fault with the regional fault system, are similar in eruptive style and magma composition to eruptions of the earlier stages of building of the volcano. The youngest volcanic activity is marked by lateral phreatomagmatic eruptions, voluminous debris avalanches, ash flow tuffs and pumice falls related to catastrophic collapse during the historic eruptions including the disastrous eruption of 1985.

Pleistocene to historic eruptive products span the compositional range from basaltic andesite to rhyodacite. Disequilibrium textures such as bimodal plagioclase, pyroxene and glass populations are evidenced especially in the dacites. Abundant low-iron amphiboles are pargasitic and seem to have crystallized in equilibrium with rare phlogopites. Crystallization temperatures from the assemblage cpx-opx and Fe-Ti oxides range between 1 175-930 °C. Basaltic andesites are only found in the Basal Unit of Ruiz. The later lavas and pyroclastic flows become progressively more evolved with time.

Acid andesites and dacites (60-65 % $SiO_2$) are the most common rock-type and show a large variability of their $K_2O$ contents. The bimodality of more evolved lavas is evidenced by their Th/Ta ratios (19-25 against 7-15) from a common source with a partial fusion giving a Th/Ta ratio near 5. Similar REE patterns for all the lavas and their major mineral phases are also consistent with a single magmatic source. However, only small differences between the lavas of the two successive phases of the building of the volcano are apparent on the multi-element spidergrams. It appears that the hiatus between the Basal Unit and the final stage corresponds to a small but significant episode : certain elements change through time, in particular LIL and HFS elements such as Rb, Ba, Th, Hf and Zr and the heavy REE increase with decreasing age. These differences probably result

*from selective enrichment due to crustal contamination. Ta-Nb anomalies are due to an incompatible-element enriched source from the sub-continental lithosphere. The source region with a Sr isotope ratio 0.704022-0.704480 reflects also a slight degree of crustal contamination and the Th/Yb-Ta/Yb ratios confirm the important role played by the subduction and the within-plate components in the magma genesis in this region.*

**Key words :** Volcanic activity - Calc-alkaline suite - Microprobe analyses - Disequilibrium textures - Major and trace elements - REE - Sr. isotope - ratios - Multielement spidergrams - Fractionation processes - Crustal contamination - Northern Andes - Cordillera Central - Colombia.

## *Résumé :* Évolution magmatique du Nevado del Ruiz, Cordillère centrale, Colombie. Chimie des minéraux et géochimie.

*Le Nevado del Ruiz, situé à 120 km à l'ouest de Bogota, est l'un des volcans andésitiques actuellement actifs et se trouve dans le nord de la Cordillère centrale de la Colombie, à l'intersection de deux systèmes de failles dominants qui trouvent leurs origines dans le soubassement paléozoïque.*

*Le soubassement pré-volcanique est constitué de gneiss paléozoïques pénétrés de batholites granitiques d'âge pré-crétacé et tertiaire. Ils sont recouverts de laves et de roches volcanoclastiques provenant d'une chaîne volcanique érodée et ravinée lors du pliocène supérieur.*

*L'histoire géologique du Nevado del Ruiz enregistre deux périodes de construction de ce volcan composite. Les relations stratigraphiques et les datations K-Ar indiquent un début de volcanisme effusif et explosif il y a environ 1 million d'années, par l'émission de laves andésitiques différenciées de coulées pyroclastiques et de dômes d'andésites selon une direction structurale régionale. La deuxième phase d'activité a débuté par des éruptions cataclysmiques. Les séquences supérieures consistent en laves chaotiques et dômes de laves de composition allant d'andésites à deux pyroxènes, à des rhyodacites. Les éruptions holocènes à récentes qui sont contrôlées par l'activité intense à l'intersection de la faille de Palestina avec le système de failles régional, ressemblent du point de vue style éruptif et composition des magmas aux éruptions des phases antérieures de la construction du volcan. L'activité la plus récente est marquée par des éruptions phréato-magmatiques latérales, d'avalanches chaotiques, d'ignimbrites et de retombées de ponces, en relation avec l'effondrement catastrophique lors des éruptions historiques, y compris celle de 1985 particulièrement désastreuse. Les produits émis à partir du pleistocène jusqu'à présent varient des andésites basaltiques jusqu'aux rhyodacites. Des textures en déséquilibre telles des populations bimodales de plagioclase, de pyroxène et de verre sont particulièrement bien représentées dans les dacites. Les amphiboles du type pargasite à faible teneur en fer abondent et ont apparemment cristallisé en équilibre avec les rares phlogopites. Les températures de cristallisation obtenues sur les thermomètres cpx-opx et oxydes Fe-Ti varient de 1 175 à 930 °C.*

*Des andésites basaltiques se trouvent seulement dans l'unité basale du Ruiz. Les laves plus récentes et les coulées pyroclastiques évoluent avec le temps. Des andésiques acides et des dacites (SiO₂ 60-65 %) sont les types de roches les plus courants et montrent une large variabilité de leurs teneurs en K₂0. La bimodalité des laves plus évoluées est mise en évidence par leurs rapports Th/Ta (19 à 25 contre 7 à 15), elles dérivent d'une source commune de fusion partielle produisant un rapport Th/Ta voisin de 5. Les similitudes des spectres des terres rares de toutes les laves et de leurs phases minérales majeures sont également en accord avec l'existence d'une seule source magmatique. Cependant, les différences qui apparaissent sur les diagrammes multi-éléments entre laves correspondant aux deux phases successives de la construction du volcan, sont seulement faibles. Il apparaît que le hiatus entre l'unité basale et l'unité terminale correspond à un épisode bref mais significatif = certains éléments varient en abondance avec le temps, en particulier les éléments du type LIL et HFS tels que Rb, Ba, Th. Hf et Zr, et les terres rares lourdes qui augmentent lorsque l'âge décroît. Ces différences proviennent probablement d'un enrichissement sélectif dû à une contamination crustale. Les anomalies en Ta et Nb sont dues à une source se trouvant dans la lithosphère sub-continentale enrichie en éléments incompatibles. Cette région dont le rapport isotopique du Sr est de 0-704022 - 0-704480 traduit également un faible degré de contamination crustale et les rapports Th-yb - Ta/yb confirment le rôle important joué par la subduction et les composants intra-plaques dans la genèse des magmas de cette région.*

**Mots-clés :** Activité volcanique - Analyses microsonde - Série calco-alcaline - Éléments majeurs et traces - Terres rares - Diagrammes multi-éléments - Processus de fractionnement - Contamination crustale - Andes septentrionales - Cordillère centrale - Colombie.

## *Resumen :* Evolución magmática del volcán Nevado del Ruiz, Cordillera central, Colombia, química de los minerales y geoquímica.

*El Nevado del Ruiz, situado 120 km al oeste de Bogotá, es uno de los más activos volcanes de la parte norte de la Cordillera Central de Colombia, a la intersección de dos importantes sistemas de fallas existentes en el basamento paleozoico.*

*El basamento ante volcanico es constituido de gneises paleozoicos cortados para los batolitos graniticos de edad pre-cretacico y tertiario, y cubierto de lavas y rocas volcano-clasticas que provienen de la destrucción, al Plioceno superior, de una cadena volcánica antigua.*

*La historia geológica del Nevado del Ruiz comprende dos épocas de construcción del volcán compuesto. Los datos estratigraficos y los edades K-Ar indican que el volcanismo efusivo y explosivo empezó aproximativamente hace 1 Ma con la erupción de coladas de lavas y piroclasticas y de domos andesiticos a lo largo de una dirección estructural regional. Erupciones cataclismicas iniciaron la segunda fase de actividad. Las secuencias superiores son constituidas de coladas de bloques y de domos que corresponden a las lavas que se tenden de las andesitas con dos piroxenos a las riodacitas. Las erupciones volcánicas que se tenden del Holoceno a la época reciente son controladas para la actividad tectonica intensa a la intersección del sistema de fallas de la Palestina con el sistema regional y son del mismo estilo y de composición magmática equivalente a las erupciones de la primera época de construcción del volcán. La más joven actividad volcánica se distingue para las erupciones freatomagmaticas laterales, los importantes avalanchas de añicos, las coladas tufaceas de cenizas y las caidas de pómez que provienen del derrumbamiento catastrófico durante las erupciones historicas como esto desastre de 1985.*

*Los productos eruptivos del Pleistoceno a la época historica se tenden de las andesitas basalticas a las riodacitas. Las dacitas mostran texturas de desequilibrio como la existencia de dos poblaciones de feldespatos, piroxenos y vidrios. Los anfiboles con hierro bajo son abundantes y de naturaleza pargasitica y parecen hacer cristalisados en equilibrio con las micas escasas. Las temperaturas de cristalización de los magmas son establecen desde las parejas opx-cpx y los oxidos Fe-Ti y se tenden entre 1 175 y 930 ºC. Las andesitas basalticas existen unicamente en la unidad inferiora del Ruiz. Las lavas y las piroclasticas más recientes se volven progesivamente más evolucionadas con el tiempo.*

*Andesitas ácidas y dacitas con 60 a 65 % de $SiO_2$ son las rocas calcoalcalinas más representadas con una variación larga de los contenidos en $K_2O$. La evidencia de la evolución brimodal de estas lavas está establicida sobre las dos trajectorias de fraccionamiento de Th y Ta (las razones Th/Ta son 19-25 contra 7-15) a partir de una fuente magmática común con una razon Th/Ta cerca de 5. Los perfiles de tierras raras, caracterisados por el enriquecimiento de las tierras livianas, son idénticos para todos los tipos de lavas. Este similitud existe también en los perfiles de las fases minerales dominantes. Estos resultados ponen en evidencia la única fuente magmática. Sin embargo, a cambio bajo pero sí significativo aparece entre la unidad básica y las secuencias superiores de construcción del volcán : las proporciones de los elementos litófilos así como las de Zr, Hf y tierras raras pesadas aumentan con el tiempo. Estas diferencias corresponden a un enriquecimiento selectivo atribuido a la contaminación crustal. Las anomalías de Ta-Nb son atribuidas al enriquecimiento de la fuente en los elementos incompatibles provenientes de la litósfera subcontinental. Por otra parte, las razones isotópicas de Sr están comprendidas entre 0.704022 y 0.704480, valores que excluyen una contribución importante de material crustal. Por último, estos resultados concuerdan con las razones Th/Yb y Ta/Yb que establecen el importante papel representado por los componentes de la subducción y de la placa continental en la génesis del magma en esta region.*

**Palabras claves :** Actividad volcánica - Análisis con microsonda - Serie calco-alcalina - elementos mayores y trazas - Tierras raras - Diagramas multielementos - Procesos de fraccionamiento - Contaminación crustal - Andes septentrionales - Cordillera central - Colombia.

# INTRODUCTION

The Nevado del Ruiz (4º50-55'N, 75º15-20'W, 5 400 m) is the northernmost and most recently active volcano of the Central Cordillera of Colombia in the Northern Volcanic Zone (NVZ = 2ºS-5ºN, THORPE *et al.,* 1984).

In this region the relative thickness of the crust is approximately 40 km and the seismic zone dips at about 20-30º to the East (HARMON *et al.,* 1984). The Quaternary Ruiz-Tolima volcanic complex lies approximately 150-170 km to the East of the oceanic trench and is built on a strongly folded Palaeozoïc metamorphic basement which is intruded by pre-Cretaceous and Palaeogene granitic batholiths (McCOURT *et al.,* 1984). The tectonics of the northern Andean block (KELLOGG *et al.,* 1985) indicate a reactivated thrust fault zone suturing accreted Cretaceous and Tertiary terranes along the western flank of the Central Cordillera, during three episodes, as summarized by MÉGARD (*in press*).

This paper focuses on some aspects of the geochemical characterization of the Quaternary to historic and Recent lavas from the Nevado del Ruiz volcano and the Pliocene volcanic formations on the flanks of
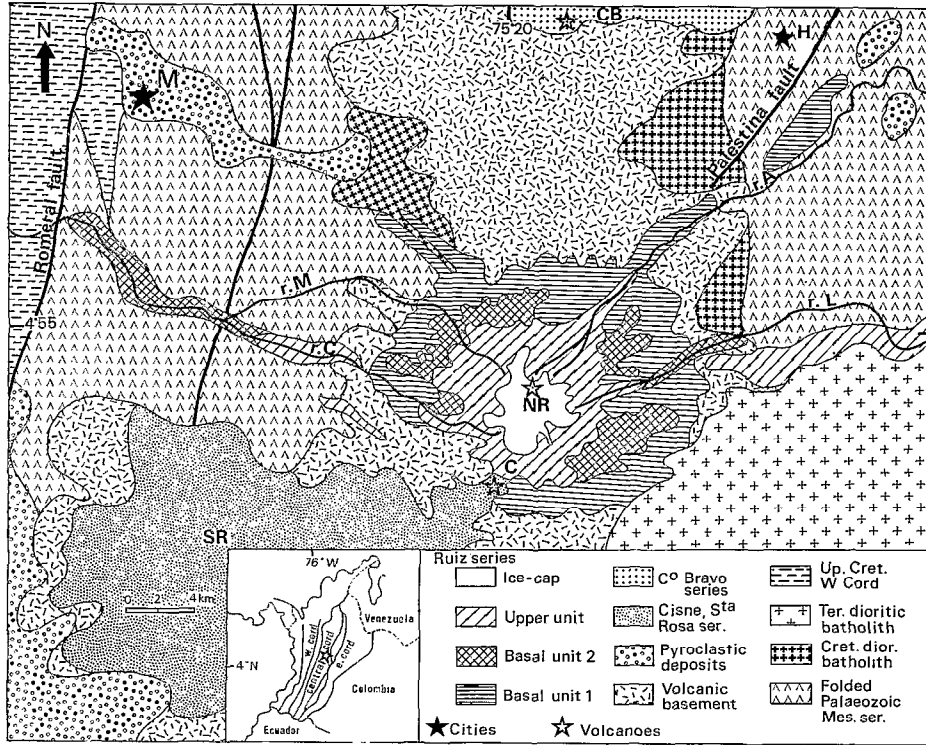
Fig. 1. — Simplified geologic map of the Nevado del Ruiz volcano *after* THOURET *et al.* (1985 c). Schematic regional geologic map from the geological map of Colombia (INGEOMINAS. 1976 b)

Abbreviations. C. Cisné. C.B. Cerro Bravo. H. Hervéo, M. Manizales, N.R. Nevado del Ruiz. r.A. rio Azufrado. r.C. rio Claro. r.L. rio Lagunilla. r.M. rio Molinos, S.R. Páramo de Santa Rosa

the Central Cordillera based on new petrological, mineralogical and geochemical data. Its main scope is to discuss the possible contamination of the magmatic source in comparison with the volcanism of the Central Volcanic Zone (CVZ) of the Andes.

## TECTONIC AND VOLCANIC HISTORY

The Central Cordillera includes over thirty Quaternary volcanoes. Seven volcanoes of the Ruiz-Tolima volcanic zone are confined to the northern 90 km-long and 20 km-wide sector, East of the accretionary *Cretaceous tectonic zone (N-S Romeral fault system)*. Here we consider only the northern half of this volcanic zone. Intense tectonic activity has concentrated several dacitic domes in this region (e.g. El Cisne) and a large volume of andesitic and dacitic pyroclastic and lava deposits has erupted from composite volcanoes, such as the Paramo de Santa Rosa and the Cerro Bravo. The Nevado del Ruiz, the more recently active volcano in the field, lies at the intersection of the

Palestina fault system (N20-30°) with the regional fault system (N120-130°) and is regarded as the most important volcano within the volcanic zone of the Central Cordillera.

**The Pliocene volcanic formations** which were emplaced before the development of the Quaternary volcanic chain have an age in the interval 4-2 Ma and consist largely of complex pyroclastic and volcaniclastic deposits derived from an old and eroded volcanic chain dissected during the late Pliocene. These formations, interbedded with voluminous andesitic and dacitic lava flows, cover the western and eastern flanks of the Central Cordillera and are exposed at two levels, in the Cauca Basin and in the Magdalena Valley.

Numerous data available on the Ruiz Volcano (INGEOMINAS, 1976a ; JARAMILLO, 1980 ; MURCIA, 1982 ; HERD, 1982) have provided valuable insights into the structure and the geochemical composition of this andesitic volcano. More recently, the field relationships have been described by THOURET (1984) and THOURET *et al.* (1985a, b, c).

The Nevado del Ruiz is classified as a compound volcano based on the identification of two distinctive phases of building. Its position at the intersection of the Palestina fault with the regional fault system suggests that the spacial focus and the composition of the volcanism, predominantly andesitic and dacitic, are controlled by the tectonic activity. Published K-Ar dates on two overlapping volcanic units (CANTAGREL et al., 1986) indicate an activity that extends through nearly 1.5 Ma.

The stratigraphy of the Ruiz volcano is summarized on Fig. 1 and only the more important features are outlined here.

**The basal unit** consists of two eruptive episodes dominated by clinopyroxene- and amphibole-andesites and biotite-dacites classified as medium-K lavas and showing a large compositional variability.

*The first episode : Basal Unit 1* (1.2-1 Ma) is characterized by a large volume of differentiated lava flows and pyroclastic deposits with clinopyroxene-basaltic andesites and amphibole-acid andesites erupted along the N20-30° dominant structural orientation (Palestina fault system).

*The second episode : Basal Unit 2* (0.8-0.6 Ma) is marked by strongly porphyritic andesites, ash and pumice flows and the growth of dacitic domes which closed this cycle.

Between this and the later phase of building, major pyroclastic eruptions took place during the periode 0.6-0.3 Ma and produced pumice and ash flow tuffs which extended to the East and West (Rio Claro). These pyroclastic flows have a mineralogy similar to that of the Pliocene pyroclastic and volcaniclastic deposits. Pyroclastic deposits of this type are commonly associated with caldera collapse in the Andean Cordillera e.g. in northern Chile (O'CALLAGHAN and FRANCIS, 1986).

The volume of magma erupted during this activity was sufficient to permit the collapse of a large caldera. Nevertheless, at Ruiz no negative gravity anomaly appears to be related to the volume of pyroclastics filling a possible caldera depression. However, BROWN et al. (1987) have shown for Costa Rica volcanoes that the low density of material filling caldera structures and topographic depressions plays an important role in the interpretation of gravity data.

The explosive activity at Ruiz appears to have increased with time, especially after the cataclysmic eruption which opened the second phase of building of the volcano in late Quaternary to Holocene times.

**The upper unit** is a young composite volcano (0.3-0.2 Ma, 0.05 Ma to Holocene), covering at least 250 km². It comprises a series of andesitic lava flows

and block lavas showing the existence of two mineralogical types : two pyroxene-andesites and amphibole-dacites or biotite-dacites. Ash flows and adventive domes are andesitic to dacitic in composition. This activity was centered on the intersection of the N30° - N120° linear structures.

The more recent volcanic history (25,000 BP to historic time) is also controlled by the intense tectonic activity at the intersection of the major fault system and marked by repeated edifice failures on the north-northeastern flank which have produced lithic pyroclastic flows and debris-flow sequences. Such an explosive vent collapsed by cataclysmic explosion on March 12, 1595 producing debris-avalanche deposits, banded pumices and ash flows.

The next major event was the 1845 phreatomagmatic eruption. This was followed by the disastrous eruption on November 13, 1985 described by HERD (1986). Relationships between the eruptive dynamism, the ice melting and the genesis of catastrophic lahars have been analysed by THOURET et al. (1987). Further description of pyroclastic flow, surge, debris-avalanche and lahars are given by NARANJO et al. (1986) and LOWE et al. (1986). Reversed magnetization in pyroclastics was observed by HELLER et al. (1986). A possible cause may be that these pumices had formed when the polarity of the earth's magnetic field had been reversed.

This suggests that pumices of the same age should have similar polarity.

Some banded pumices from fall deposits are considered by WILLIAMS et al. (1986) as accidental and coming from old magma compositionally similar to historic pyroclastic deposits.

## ANALYTICAL METHODS

Samples were collected from pyroclastic sequences and massive lava flows and analytical techniques for each sample are reported in table VIII.

Only twelve samples of pumices and lavas were chosen for determination of mineral, glass and matrix compositions, plus an additional two pumices analysed by A. GOURGAUD, University of Clermont-Ferrand (THOURET et al., in press) from the 1985 eruption. All mineral analyses (tables I to VII) were performed on a CAMECA-CAMEBAX electron microprobe at the Laboratoire de Géologie, University of Clermont-Ferrand, under routine run conditions, using conventional wavelength and energy dispersive methods.

Thirty-two lava and pumice samples from the major eruptive sequences of the Ruiz volcano and the volcanic piedmont formations, plus fourteen pumices from the 1985 eruption sampled by Colombian and Spanish colleagues, were analysed for major elements using energy-dispersive X-ray fluorescence

*(EDXRF)* at the Laboratoire de Géologie, University of Grenoble, or Atomic Absorption (AA) at the Laboratoire de Géologie, University of Clermont-Ferrand (table VIII).

Seventeen pumices and lavas (tables IX and X) have been further analysed for Rare Earth Elements (REE) plus Ta, Hf, Th, U, Sc and Cs by Instrumental Neutron Activation Analysis (INAA) at the Institut Laüe-Langevin (ILL), Grenoble, following the experimental conditions and procedure contained in ILL Experimental Report 03.13.21 (OLIVER and KERR, 1981) and Nb, Zr, Ba, Sr, Y and Rb by XRF at the Laboratoire de Géologie, University of Lyon. Mineral separates and groundmasses of two contrasted pumices ejected from the 1985 eruption were also analysed for REE by INAA (table X).

Eight isotopic determinations of Sr were made at the Laboratoire de Géochimie Isotopique, University of Montpellier, by L. BRIQUEU (table XI) using the method described in BRIQUEU (1985) and BRIQUEU *et al.* (1986).

## PETROGRAPHY

Most lavas and pyroclastic flows of the Ruiz volcano as well as the volcanic piedmont formations are restricted to a narrow compositional range. It is possible to recognize a calc-alkaline suite subdivided into moderate-K and high-K facies. The most useful criterium is ferromagnesian phenocryst mineralogy. This Ruiz suite consists of about 40 % dacites and 60 % andesites (VATIN-PÉRIGNON *et al.*, 1987b).

The andesitic lavas from the *Pliocene volcanic piedmont formations* contain about 30 % phenocrysts and are characterized by plagioclase An 60-48 + augite - salite Wo 46-44 En 46-41 Fs 14-9 + bronzite En 88-81 ± hornblende in a microlitic groundmass composed of plagioclase, pyroxene and titanomagnetite. The basaltic andesites of *Basal Unit 1* consist of phenocrysts of plagioclase An 65-70 (50 %) and augite (10 %) in a fine-grained to doleritic groundmass composed of intergranular augite, magnesian olivine and titanomagnetite. Two-pyroxene porphyritic andesites are well represented with a dominant mineral assemblage of plagioclase An 60-40 and An 50-35 with normal oscillatory zoning + clinopyroxene Wo 40-En 45 + titanomagnetite (Usp 28, Ilm 37) + orthopyroxene En 65-68 or En 75-83.

The *Basal Unit 2* and the *Upper Unit* vary in composition from acid andesites to dacites with mineral assemblages consisting of plagioclase An 35-55 + orthopyroxene En 75-78 + amphibole or biotite + titanomagnetite (Usp 22-30, Ilm 30-40) + clinopyroxene Wo 43 En 41 ± olivine Fo 80-87.

In the pumice and ash flow deposits from *major historic events*, plagioclase An 40 occurs both as phenocrysts and in glomerocrysts with augite Wo 40

En 43 Fs 17, bronzite - hypersthene En 70-65, titanomagnetite He 36-33 in a rhyolitic glass. The hornblende is always surrounded by magnetite or totally reacted to granular opaque minerals. Devitrified areas of the glassy groundmass contain secondary mineralogy (zeolites and hydrated aluminosilicates, micas and hematite). Modal analysis gives : plagioclase 50 %, orthopyroxene 17 %, clinopyroxene 3 %, resorbed amphibole 2 %, titanomagnetite 8 %, groundmass glass 20 %.

Significant mineralogical differences are apparent in the lavas of other volcanoes in the vicinity of the Nevado del Ruiz. Pliocene andesites from the Paramo de Santa Rosa volcano are in the two-pyroxene range. The andesites of the Quaternary dome of Cisné are characterized by the phenocryst assemblage : plagioclase + clinopyroxene + amphibole. Orthopyroxene is rare. Amphibole is also a relatively abundant phenocryst phase in andesites and dacites of the Holocene Cerro Bravo volcano and coexists with plagioclase and orthopyroxene. These lavas and pumices also contain xenolithic granodioritic fragments, small amounts of quartz and relict olivine phenocrysts with pyroxene reaction rims.

## MINERAL CHEMISTRY

### Feldspars

The composition of feldspar in phenocrysts and microlites ranges from An 30-60 in dacites and andesites with significant K contents (Or 1.5−8.9, table I, fig. 2). Whole rock $K_2O$ equal or more than 2.5 % in andesites from the *Basal Unit* showing a high-K calc-alkaline tendency, is not correlated with Or contents of plagioclase.

Different compositional variations have been found in calc-alkaline rhyodacitic series from Mexico (MAGONTHIER, 1984) and the CVZ in the Andean (GOEMANS, 1986, GOEMENS et al. 1987a, b). High or contents (more than 5 %) of plagioclases are unusual in the Ruiz lavas and such feldspars only occur as isolated phenocrysts or crystallites in the matrices of some recent pumices.

The normal variation among individual phenocrysts ranges from An 58, 56 to 43, 32 in dacites to An 51, 48 to 42 in andesites. The presence of bimodal plagioclase population : (1) normally zoned phenocrysts, (2) 10 to 30 mole % reverse zoning from the andesitic piedmont formations to historic dacitic pyroclastic sequences, is always accompagnied by amphibole phenocrysts showing various stages of breakdown.

### Pyroxenes

Andesites and dacites contain augite phenocrysts with a restricted range of Mg* (100 Mg/Mg + Fe t)

=72 to 78 (table II (A), fig. 3). More calcic augitic clinopyroxenes are found in andesitic lavas and pyroclastic flows which have approximately the same whole-rock composition. Mg-rich clinopyroxenes with a limited range of Mg* = 84 to 86 only occur as microphenocrysts in the pumice flows from the Holocene pyroclastic sequences.

Orthopyroxenes show more compositional variation than clinopyroxenes (Mg* = 67 to 90, table II (B), fig. 3). Two types of orthopyroxene crystals are founds in various pumice flows : large crystals of hypersthene which contain Ti-oxide inclusions and small euhedral crystals or broken crystals of bronzite. Bronzite occurs in Pliocene andesites and hypersthene in black andesitic pumices from the *Upper Unit* of the Ruiz volcano ; Mg-pigeonite phenocrysts are rare and occur possibly in equilibrium with augite and hypersthene in the dacitic component of the 1985 eruption (THOURET *et al., in press*). Two pyroxene temperatures (WOOD and BANNO, 1973) from the assemblage cpx-opx (tables II (A and B) ) give 1 164 °C ± 50 °C (cores) for Holocene dacitic pumices. Analyses of coexisting cpx-opx in historic andesitic pumices yield temperatures of 1 174 °C ± 50 °C (cores) and 1 158 °C ± 50 °C (rims). The accuracy of these values within the uncer-
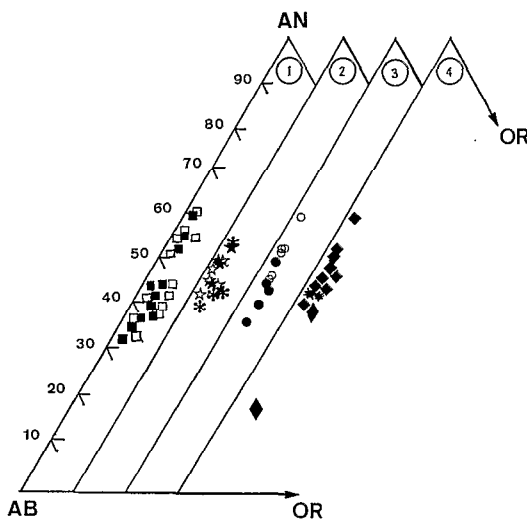
Fig. 2. — Plagioclase compositions in normative Ab/Or/An diagram (Table I)

1 : 1985 deposits (dacitic pumices : full square ; andesitic pumices : open square)
2 . historic eruptions (83-212 · full star ; 83-212a : open star ; 83-227 asterisk)
3 · Holocene eruptions (83-111a : open circle . 84-27a  full circle)
4 . Upper Unit (83-186 : elongated full diamond) ; Basal Unit (83-255   large asterisk) ;
Pliocene volcanic piedmont formations (83-273 · full diamond)
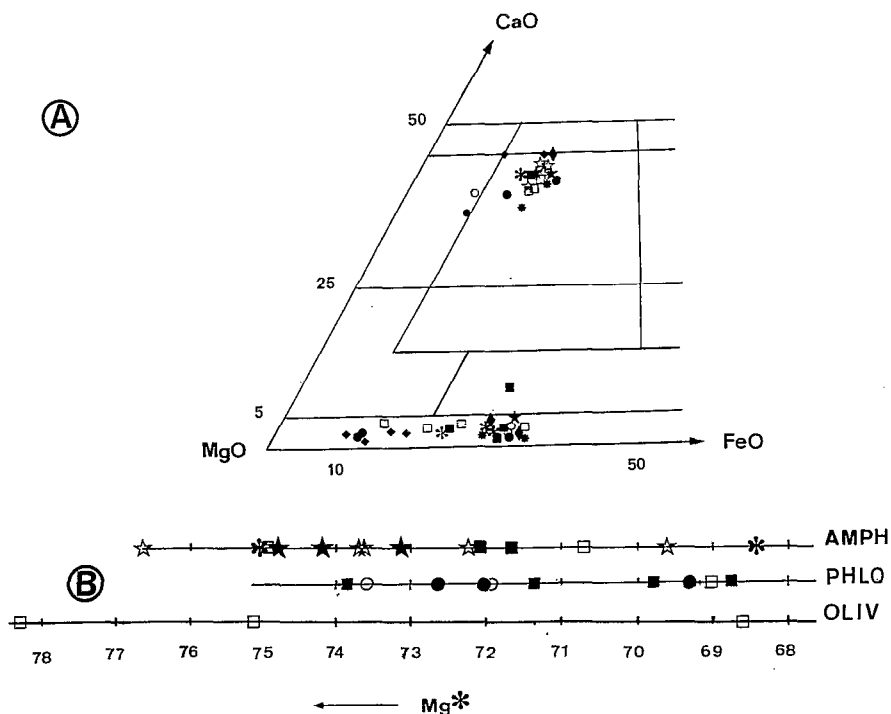
Fig. 3 A. — Pyroxene compositions in Cao/MgO/FeOt diagram (oxide wt. %, Tables II (A) and (B) ). Total Fe as FeO ; symbols as in Fig. 2
3 B. — Mg* variation diagram for amphibole, phlogopite and olivine compositions (Tables III, IV and V). Mg* = 100 Mg / Mg + Fe t. (Calculation on the basis of 23 oxygen atoms for amphibole, 24 for phlogopite and 4 for olivine). Symbols as in Fig. 2

tainties of the geothermometer appears not significant as discussed by d'ARCO (1982). Average temperatures from coexisting opx-cpx from pyroclastic flows (Upper Unit) are generally similar to those from Holocene and historic eruptions and show small variabilities. The temperatures obtained, relative to the Wood-Banno geothermometer, are higher than those expected for pumice pyroclastic flows. Nevertheless, these results appear as consistent with temperatures estimated by a graphical thermometer applied to augite-orthopyroxene pairs (LINDSLEY, 1983).

## Amphiboles

Amphibole is a common phenocryst phase (8 to 12 % of phenocrysts) in the lava flows from Basal Unit 2. Most of the amphibole phenocrysts are typically rimmed by reaction coronas of black alteration (oxidation) showing relict cores sometimes resulting in a complete pseudomorphs.

In the products from the 1985 eruption, amphibole occurs only as unzoned phenocrysts (THOURET *et al., in press*). Differences are seen between phenocrysts in the white pumice HC41 (edenite following LEAKE, 1978) and those in the brown pumice HC42 (pargasite, table II, figs 3 (B) and 4 (A) ) ; in these low-iron amphiboles, the cation contents refer to 23 anhydrous oxygens and the stoichiometric assumptions (ROBINSON *et al.,* 1982) are « all FeO » and total cations to 13 exclusive of K, Na, Ca and Mn. The composition of the amphiboles from the 1985 brown pumices is

similar to that observed in other pyroclastic products from historic eruptions and the majority of amphiboles fall within the pargasite field. In all these amphiboles, the increase in Si (6.0 to 6.8) shows no correlation with an almost constant Mg* (68 to 77, fig. 3 (B) ). In Fig. 4 (B), a large hyatus appears between the edenite type, with a moderate Al content, and the pargasite type in which there is a significant amount of tetrahedral Al substituting for silica. Pargasite and edenite amphiboles have Na + K = 0.70 to 0.83. The pargasite contents range from 70 to 85 % with 20 % of the edenite molecule. The alkalinity of the white pumice HC41 (anal. 46, table VIII and fig. 7) : $K_2O = 3$ %, similar to high-K calc-alkaline series, is reflected by the potassic nature of edenite ($K_2O = 0.85$ to 0.94 %). Amphiboles from both historic and the last eruption show no sensitivity to rock composition : pargasite from acid andesites with more than 6 % CaO in the rock contain 1.7 to 1.8 Ca, the same as edenite from the dacite HC41 with less than 5 % CaO.

## Mica

Mica is not an important phase. Phenocrysts are generally scarce, small and fresh in dacitic lavas from the Upper Unit whereas large mica plates with reaction rims are observed in all the porphyritic lavas from the Basal Unit.

In pyroclastic deposits, mica occurs as phenocrysts and can show partial resorption. Representative mica compositions from both Holocene and the 1985 pyroclastic deposits are listed in Table IV. All micas
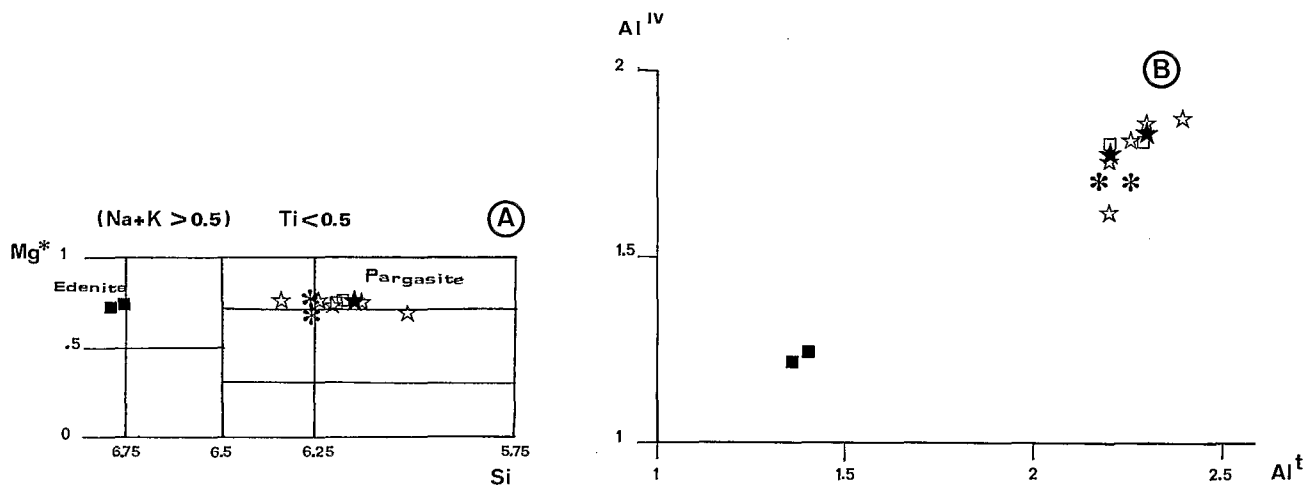


Fig 4 A. — Amphibole compositions in LEAKE diagram (1978) (Table III). Mg* = Mg/Mg + Fet. Amphibole formulae are established on the basis of the chemical and crystal-chemical limits (ROBINSON *et al.,* 1982). Formulae for calcic amphiboles are most satisfactory using all FeO and 13 cations. The 13 cations assumption excludes K, Na, Ca and Mn (STOUT, 1972). The Na is distributed between the A-site (with K) and the B-site (with Ca) as seems to be common in many calcic amphiboles
4 B. — Al$^{IV}$ vs Al t Al$^{IV}$, Al t, Na, K and Ca calculated on the basis of 23 oxygen atoms

have Mg/Fe ratios > 2 corresponding to phlogopites. Variations in Mg/Fe (2.2 to 2.8) and in Mg* (69 to 73) indicate a restricted compositional field. Mg and Si content variations in phlogopites take place with Al*almost constant (2.3 to 2.6) characterizing their homogeneity. The ratio of Mg amphibole / Mg phlogopite (after Mg contents from tables III and IV) is equal to or greater than unity and these two minerals would appear to have crystallized in equilibrium.

## Olivine

Olivine is present in some of the basaltic andesites either as microphenocrysts or grains associated with titanomagnetite. In all cases crystals are too small to be accurately analysed or have been extensively altered by late-stage oxidation processes.

In dacitic lavas from all units, olivine crystals show evidence of disequilibrium with important reaction rims. In aggregates from historic dacitic pyroclastic sequences, olivine rimmed by orthopyroxene coexists with amphibole, titanomagnetite and glass.

Olivine from the 1985 eruptive products is rare and only found as individual crystals in glomeroporphyritic aggregates or as corroded core phenocrysts mantled with hypersthene (THOURET et al., in press). Representative olivine compositions are listed in Table 5. A common feature is simple normal zoning from Fo 87-84 cores to Fo 79 rims. More important variations exist between the Mg numbers of olivine (78 to 68) than those of phlogopite and amphibole (fig. 3 (B) ). Percentages of Ca are less than 0.15 %.

## Fe-Ti oxides

Titanomagnetite and ilmenite are common phases in all the lavas and pyroclastic deposits and occur in close association as phenocrysts, small grains in the groundmass or inclusions in mafic minerals. Oxides in glomeroporphyritic assemblages are typically associated with pyroxene and glass. In some lava flows from the Basal Unit 2, cumulates consisting of pl + opx (50 %), glass (10 %) and intercumulus Ti-Fe oxide (40 %) occur. Representative analyses of titanomagnetite and ilmenite are presented in Tables VI (A) and VI (B).

In pumiceous pyroclastic sequences from Holocene to recent times, eruptions containing coexisting titanomagnetite and ilmenite, Usp calculated by the method of CARMICHAEL (1967) lie between 17 and 35 mol% ; however, two titanomagnetite populations are found : one with 1.5 to 3.2 % MgO and 1.5 to 3 % $Al_2O_3$ and another with up to 3.7 % MgO and 3.2 % $Al_2O_3$ (anal. 6 and 7, table VI (A) ). Ilmenite compositions with He 30 to 43 mol% are similar in all pyroclastic units.

Although andesites and dacites show low-$TiO_2$ contents (0.42 to 0.88 %), ilmenite phenocrysts are present in some andesitic lavas from the Pliocene volcanic formations (anal. 16, table VI (B) ), but low MnO contents (close to 0.5 %) indicate no alkaline tendency.

Calculated Fe-Ti equilibration temperatures (POWELL and POWELL, 1977) for composite grains included in cpx from historic pyroclastic eruptions (968-1 029 °C ± 50 °C) or for microlites (990-1 051 °C ± 50 °C) are systemacically lower than opx-cpx equilibrium temperatures (1 174-1 158 °C ± 50 °C). Holocene pyroclastic flows have magmatic temperatures (933-1 033 °C ± 50 °C for phenocryst cores ; 1 020 °C ± 50 °C for small grains) in good agreement with temperatures reported for two-pyroxene ande-
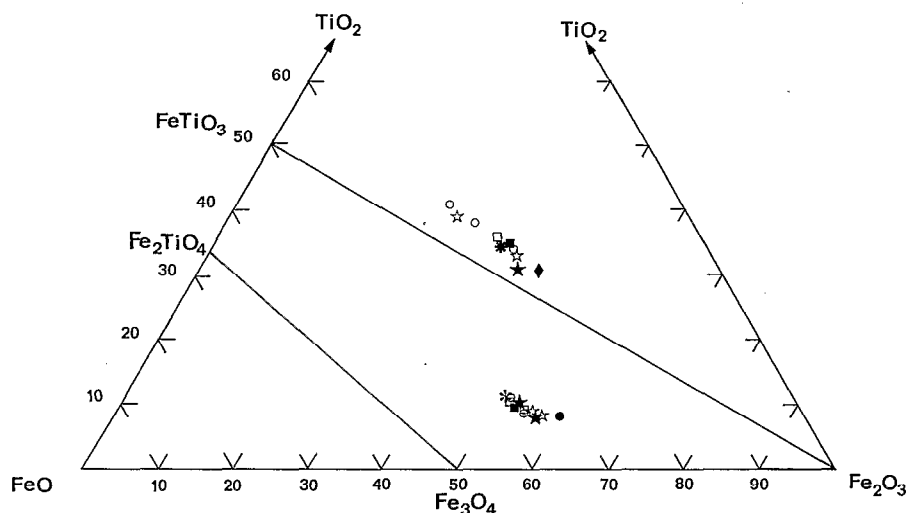


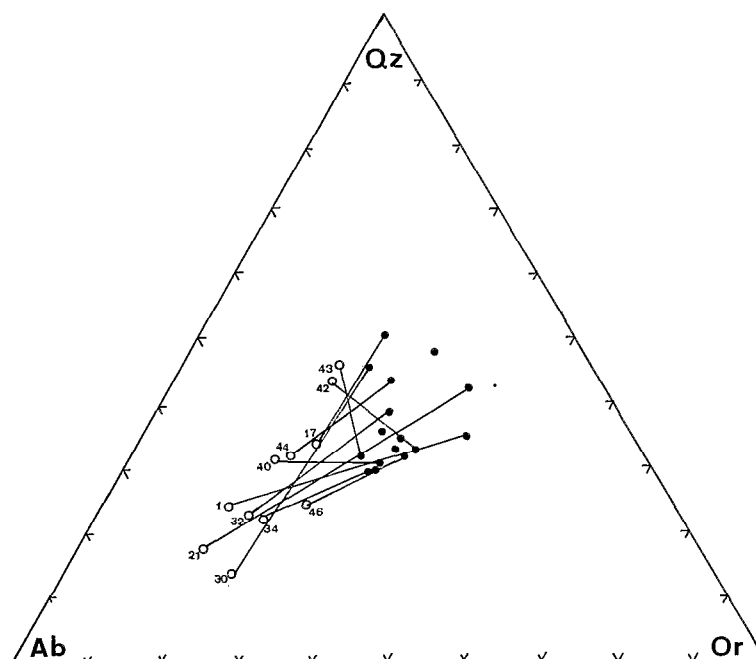Fig. 5. — FeO/$Fe_2O_3$/$TiO_2$ diagram for Fe-Ti oxides (wt.%, Tables 6 (A) and 6 (B). Symbols as in Fig. 2

Fig. 6. - Normative Qz/Or/Ab diagram showing whole-rock (open circle) / glass (full circle) pairs for 11 Ruiz pumices from the Pliocene volcanic formations th the 1985 eruption. Sample numbers refer to samples whose chemical analyses are listed in Table VIII

sites (between 950° and 1 100 °C, GILL, 1981, p. 65).

On a *TiO₂-Fe₂O₃ diagram* (fig. 5) titanomagnetites and ilmenites do not plot on BUDDINGTON and LINDSLEY equilibrium curves (1964) suggesting Al-Mg spinel intervention as recognized in another Andean context (GOEMANS, 1986).

## Accessory minerals

Apatite is rare and occurs as microphenocrysts and inclusions in amphibole in dacites.

Zircon and sphene are present, in small amounts, in mineral separates from pumice powder analysed for REE by INAA.

## Groundmass and glass

Many of the lavas show a microcrystalline groundmass with interstitial glass ; different types of glassy matrix and glassy walls of vesicles are present in pumiceous pyroclastic flows.

Glass and the glassy matrix (table VII) are compositionally bimodal. Pumices from the 1985 eruption reveal the variability of composition of the glass ; the matrix of dacitic pumices consists mainly of rhyolitic colorless glass (anal. 1 to 5), whereas dacitic brown glass is usually present in the matrix of andesitic

pumices (anal. 6 to 9). Rhyolitic glass with small compositional differences is also found in the matrix of Pliocene and Holocene vesiculated pumices. Other types of matrix and glass are compositionally intermediate between the rhyolitic and the dacitic types.

FeO* contents in glass vary from 0.5 to 4.7 % and Na₂O/K₂O from 0.3 to 1.3. Less differentiated glass appears with high FeO* and Na₂O/K₂O close to unity, whereas chemical similarities, such as low FeO*contents and Na₂O/K₂O ratios systematically less than unity, are apparent between all the other, more evolved, glass types.

The majority of evolved glasses shows a normative An content ranging between 2 % and 7 % ; the dacitic glasses are characterized by a normative An content in the range 12-20 %.

This contrast between the glass and the whole-rock composition decreases from the Pliocene formations to the historic eruptions, as seen in the *normative Qz-Or-Ab diagram* (fig. 6) whereas a change appears in the positions of tie-lines between the 1985 pumices and their glass compositions.

The more porphyritic pumices are significantly Ab-enriched and their position correspond to the abundance and composition of the phenocryst phase.
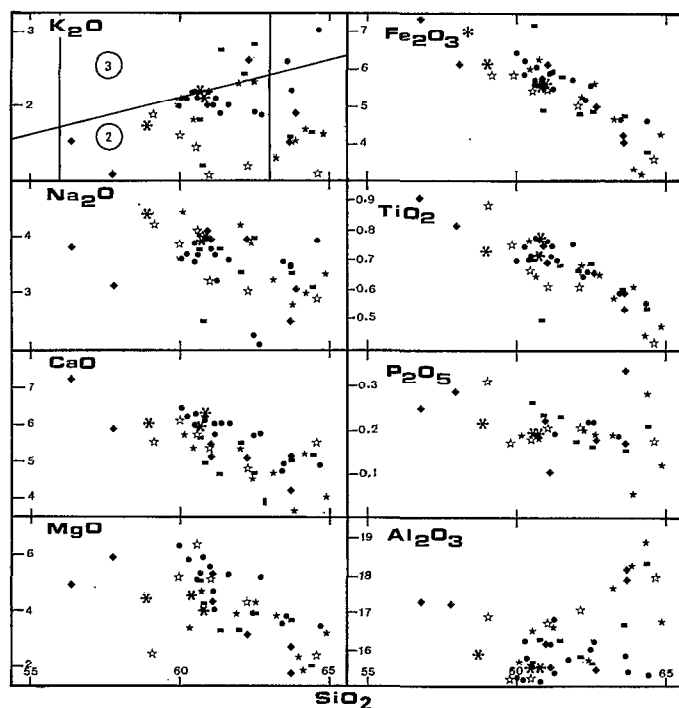
Fig. 7. — Major-element variation diagram for 46 representative lavas and pumices from the Nevado del Ruiz volcano and the Pliocene volcanic piedmont in weight per cent

Lines on the K2O diagram show the boundaries between the « normal »-K calc-alkaline series (2) and the high-K calc-alkaline series (3) after PECCERILLO and TAYLOR (1976)
Pliocene volcanic piedmont formations . open star (6 samples)
Basal Unit 1 : full diamond (7 samples)
Basal Unit 2 : full rectangle (7 samples)
Upper Unit : full star (9 samples)
Historic eruptions : asterisk (3 samples)
1985 pyroclastic deposits . dot (14 samples)

## GEOCHEMISTRY

### Major elements

Forty-six representative analyses of lavas and pumices belonging to the various eruptive sequences of the Nevado del Ruiz and the Pliocene volcanic piedmont formations are shown in table 8. A striking feature of the Ruiz lavas is their restricted range of $SiO_2$ content with 92 % of them in the interval 60 to 65 % $SiO_2$. However, this is probably due to the fact that products of the historic and the 1985 eruptions constitute most of the analyses available at present.

The products of the eruptive activity as a whole, are typically calc-alkaline in character, as seen in the $K_2O$ vs $SiO_2$ diagram (fig. 7). The majority of lavas and pumices fall within the « normal »-K field of PECCERILLO et TAYLOR (1976), whereas only a few samples (including 3 pumices and 3 lavas from all stages of the volcanic activity), fall within the high-K series field. The distinction between these two fields being by nature arbitrary, it can be said that the Ruiz data only

show a large variability of their $K_2O$ contents. A dominant group at approx. 61 % $SiO_2$ corresponds to lavas with a porphyritic texture, having abundant phenocrysts (more than 30 % modal). This group also corresponds to the highest values of $K_2O$ between 1.8 and 2.3 %. Smaller $K_2O$ values at about 1.6 % and 64 % $SiO_2$ correspond to aphyric lavas.

On other variation diagrams, dispersion in the element distribution is less apparent and a general negative correlation is observed between $SiO_2$ contents and CaO, MgO, $Fe_2O_3$* and $TiO_2$ contents. $P_2O_5$ and $Al_2O_3$ vs $SiO_2$ are not significant. It could be said however, that these variation diagrams express the minor differences observed between the eruptive products of the Ruiz volcano and the underlying Pliocene pyroclastic formations which show lower $K_2O$ and $Fe_2O_3$* contents.

### Trace elements

Determinations of RE and a number of trace elements have been made on 17 lavas and pumices correspon-
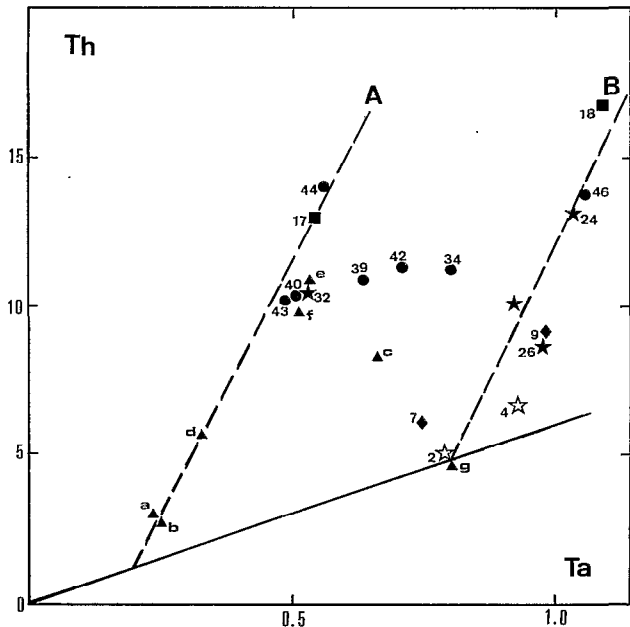
Fig 8. — Th vs Ta (ppm) diagram showing two fractionation trends (A) and (B)

Data and sample numbers listed in Table IX (same symbols as in Fig 7)
Full triangle : a to d : data from MARRINER and MILLWARD (1984).
e to g data from JARAMILLO (1980)

ding to both older (Pliocene) and younger (Pleistocene to Recent) phase of the volcanic activity (table IX).

A discriminant diagram (fig. 8) of *Th against Ta* suggests two of the major questions to be asked about the Nevado del Ruiz volcanics. These questions are : a) what and where is the source of the magma ? b) what evolution has it subsequently undergone ?

Two basaltic andesites : *sample a*, from MARRINER and MILLWARD (1984), and *sample g*, from JARAMILLO (1980) represent the most primitive magmas erupted at Ruiz. These two old olivine-basaltic andesites have been used as possible parental magmas in the discussion that follows.

It can be seen from this diagram that the Ruiz lavas have a common source with partial fusion giving a Th/Ta ratio of approximatly 5. In each unit, andesitic and dacitic pumices have specific incompatible trace element signatures. Pumices with Th/Ta ratios from 19 to 25 plot along or near the trend line (A) extrapolated from the basaltic andesite (a), characterized by a Th/Ta ratio close to 14. On the trend (B) extrapolated from the basaltic andesite (g) with a lower Th/Ta ratio (5.7), a second group is distinguished by its relatively lower Th/Ta ratio (7-15). A significant portion of the pumices erupted during the 1985 eruption corres-
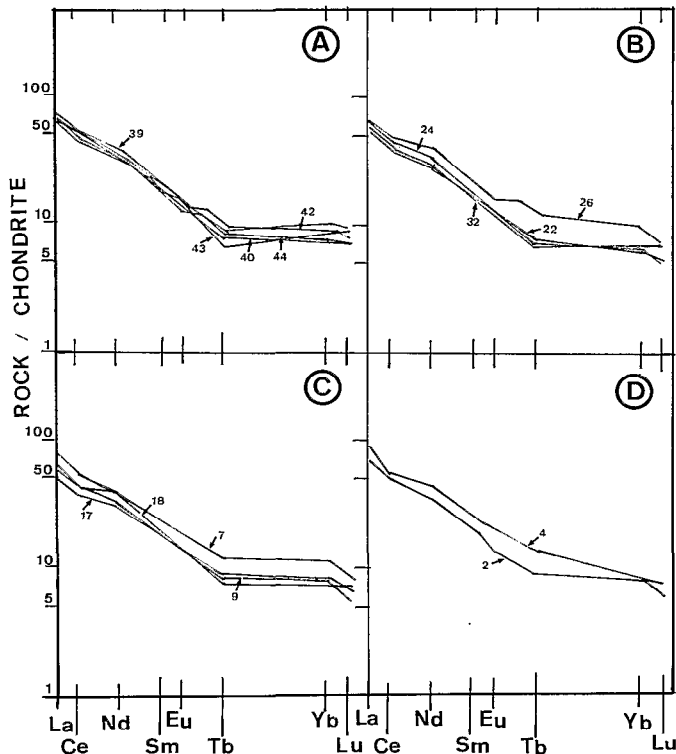


Fig. 9. — Chondrite-normalized (C[4]. NAKAMURA, 1974) REE patterns of selected lavas and pumices (Table IX)
A : 1985 pyroclastic deposits (5 samples)    C . Basal Unit 1 and 2 (4 samples)
B : Upper Unit (3 samples) and historic eruption (1 sample)    D : Pliocene volcanic piedmont formations (2 samples)
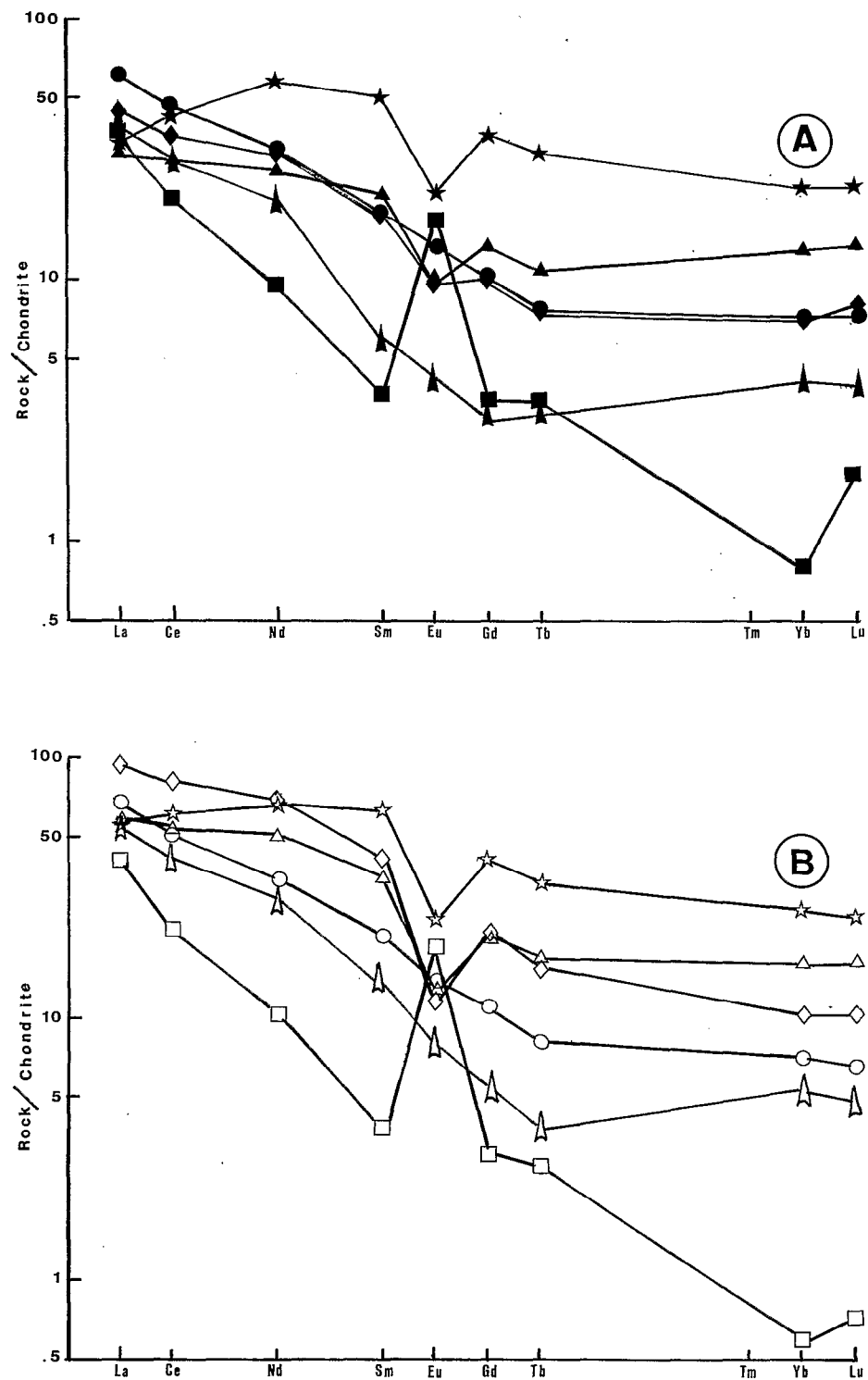
Fig. 10. — Chondrite-normalized REE patterns of pumices (whole-rock, separated minerals and groundmass, Tables IX and X)

A · andesitic brown pumice HC42 (full symbol)
B : dacitic white pumice HC41 (open symbol)
circle . whole-rock, square · feldspar, diamond : magnetite, triangle orthopyroxene. star : clinopyroxene, arrow : groundmass.
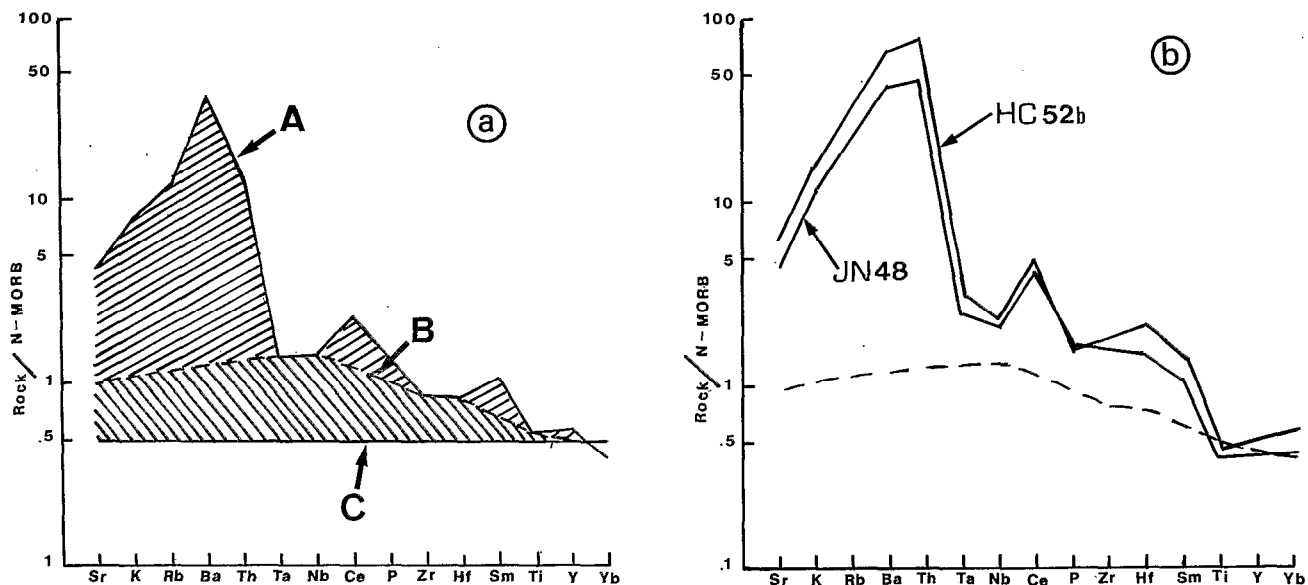
Fig. 11 — Multi-element spidergrams normalized to N-Type MORB (PEARCE, 1983) for an andesite from the older volcanic sequence of the Ruiz volcano (a) and two contrasted pumices from the 1985 eruption (b)

A representation of the basaltic andesite MB 257A, the most mafic lava of Ruiz (from MARRINER and MILLWARD, 1984).
B initial composition of the lithospheric material.
the residu (A - B) gives the component of contamination due to the subduction zone.
C composition of the primitive N MORB
(K, P and Ti in oxides %, other elements in ppm)

pond to a mixture of the two contrasted varieties. This strongly suggests that this is a bimodality of the fractionation processes of the products of the Ruiz volcano.

There common source is emphasized by chondrite-normalized plots of the *rare earth elements (REE) data* (fig. 9), which show a marked enrichment of the light REE whilst the heavy REE have some degree of enrichment, e.g. 8 times chondrite values, and are very flat lying. All the Ruiz lavas have remarkably similar REE patterns without Eu anomalies (VATIN-PÉRIGNON *et al.*, 1985). The enrichment in REE, especially the heavy REE content of dacite from the Upper unit (sample 26, fig. 9 B) could be due to the role played by the accessory phases in these more evolved liquids, but could also indicate a higher rate of fusion from a garnet rich source. However, two-pyroxene andesites of the Pliocene pyroclastic piedmont formations and of the Basal Unit 1 (sample 4 and 7, fig. 9 C and D) show higher concentrations of LREE than the dacites suggesting that these two formations are consanguineous and that *slight but significant change in the rate of fusion took place before the building of the young composite volcano.*

It is interesting to note that the patterns of andesitic and dacitic pumices lie very close together and well within the spread of all samples.

This homogeneity is further evidenced by the *patterns of mineral separates* (fig. 10, tables IX and X) from two contrasted pumices which have nearly identical patterns for major mineral phases : plagioclase, orthopyroxene and clinopyroxene. Iron-titanium oxides show small variations. The $TiO_2$-rich magnetite forms the dominant population in the white pumice HC41 (B). The pattern of this mineral clearly reflects the negative Eu anomaly of ilmenite.

Turning now to the question of a possible origin and/or an eventual contamination of the source material, spidergrams after PEARCE (1983) have been plotted. The pattern obtained on fig. 11 (a) is typical of this sort of geotectonic setting from the Central Andes (DOSTAL *et al.*, 1977 ; HAWKESWORTH *et al.*, 1982, BOILY *et al.*, 1983, GOEMANS, 1986) and the Southern Andes (THORPE *et al.*, 1976, LOPEZ-ESCOBAR, 1984, HARMON et al., 1984) with a progressive enrichment of Large Ion Lithophile (LIL) elements : K, Rb, Ba and Th and a marked positive Ce anomaly.

This is born out in *spidergrams of two pumices from the 1985 eruption* (fig. 11, b). N-MORB normalized LIL and High Field Strengh (HFS) elements such as Zr, Hf and Nb and HREE are uniformly lower in the two-pyroxene andesite (JN48) than in the biotite-dacite (HC 52b), while Ce and P remain unchanged. However, the minor positive anomalies of Ta, Nb, Zr and Hf are most probably due to an incompatible-element enriched source from the sub-continental lithosphere.
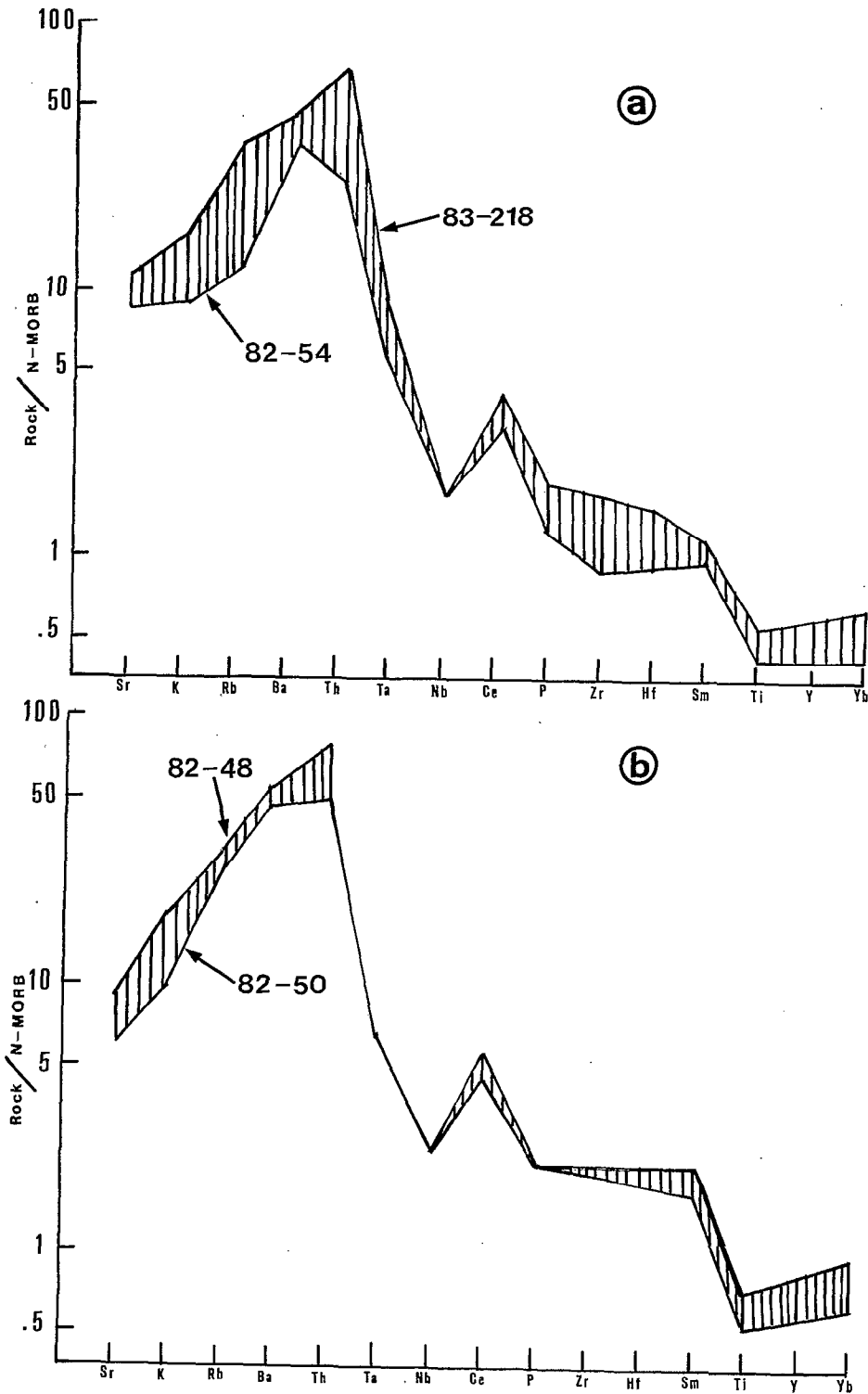
Fig. 12. — Multi-element spidergrams normalized to N-Type MORB (PEARCE, 1983) for the Basal Unit 1 and 2 (a) and the Upper Unit (b) from the Ruiz volcano

Enclosing hatched fields represent analysed lavas of each formation (Tables 8 and 9) :
82-54 Basal Unit 1 (sample n° 7) , 83-218 : Basal Unit 2 (sample n° 18) ; 82-48 and 82-50 : Upper Unit (samples n° 22 and 26)

Similar Nb-Ta anomalies in magmas associated with subduction zones have been discussed by BRIQUEU *et al.* (1984).

The *multi-element spidergrams* summarize the variations in the enrichment/depletion trends of the Basal and Upper Units (fig. 12 A and B). Acid-andesites and dacites from the Upper Unit have similar concentrations of HFS elements Ta, Nb, P and little variation of LIL and other elements. However, concentration ranges of all elements plot within the andesite-dacite field of the Basal Unit. These spidergrams which have very similar profiles, reinforce the hypothesis of an origin from an enriched mantle source and also indicate that there has been very little evolution through the last one Ma.

## Sr Isotopes

The variation of $^{87}Sr/^{86}Sr$ with $SiO_2$ in the Ruiz suite is compared to other suites from the Northern Volcanic Zone (NVZ : Ecuador) and the Central Volcanic Zone (CVZ, southern Peru, northern Chile) (table XI and fig. 13a). The Ruiz association shows $^{87}Sr/^{86}Sr$ ratios (0.704022-0.704480) which coincide with those of Ecuadorian andesites (FRANCIS et al., 1977). As shown by MARRINER and MILLWARD (1984), in both cases, there is no significant increase in Sr isotope ratios with differentiation : This suggests that these associations evolved from a source region at 0.704 (trend 1), slightly enriched and the displayed patterns of Sr isotope ratios indicate that there has been little crustal contamination. Similar volcanic rocks from other areas (northern Chile, southern Peru) have their trends parallel but slightly higher than those from the NVZ (Ecuador, Colombia). Their source region appear in the range of 0.706 (trend 2) as discussed by HAWKESWORTH *et al.* (1982) for the San Pedro-San Pablo volcanic area (northern Chile, field C).

This reflects variations in the degree of crustal contamination for the NVZ and CVZ, as evidenced by other isotopic studies (JAMES, 1984 ; HARMON *et al.*, 1984) and on a $^{143}Nd/^{144}Nd$ versus $^{87}Sr/^{86}Sr$ diagram by BRIQUEU *et al.* (1986). A plot of Sr/Nd against $SiO_2$ (fig. 13b) indicates the similarity between the northern Colombian (A), Ecuadorian (B) and northern Chilean (San Pedro-San Pablo (C)) volcanic sources (LOPEZ-ESCOBAR, 1984) whilst intrinsic differences have been observed with southern Peruvian (D) and northern Chilean (Purico (E)) parental magmas. Likewise, at Ruiz a continuing phenomenon would have occurred through time from late Cenozoic to Holocene, but the possible degree of crustal contamination could be significantly lower than the one proposed by JAMES and MURCIA (1984).

Lavas from the Ruiz volcano plotted on the *Th/Yb versus Ta/Yb diagram* (fig. 14) show an overlap between northern Colombia and the Central Andes (A). However, significantly higher Th/Yb ratios can be
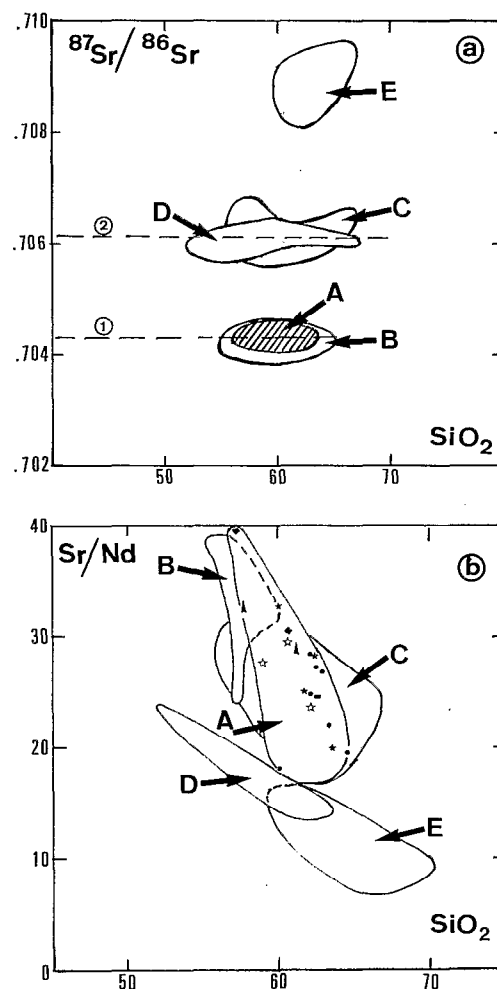


Fig. 13. — Sr isotope ratios and Sr/Nd versus $SiO_2$ for andesites and dacites from the Ruiz volcano (Tables VIII and XI). a : $^{87}Sr/^{86}Sr$ versus $SiO_2$ for volcanic suite from Ruiz (A) compared to data for Ecuador (B) (FRANCIS *et al.*, 1977), San Pedro-San Pablo, N. Chile (C) (THORPE *et al.*, 1976), Solimana, S. Peru (D) (GOEMANS, 1986), Purico, N. Chile (E) (HAWKESWORTH *et al.*, 1982). Horizontal trends (1) : 0.704, (2) : 0.706 : b ᐧ Sr/Nd versus $SiO_2$
Symbols as in Fig. 7. arrow : data from MARRINER and MILLWARD, 1984

seen in the more recent lavas from Ruiz (table IX, Upper Unit of the Volcano and the 1985 eruption). The fractionation trends (PEARCE, 1983), extrapolated from the Basal Unit 1 of Ruiz and the Pliocene volcanic formations, confirm the parts played by subduction (s) and within plate (w) components during its two distinctive phases of activity.

These findings lead us to propose a dynamic situation beneath the Ruiz volcano along the following lines. A sub-continental mantle source of magma is generated, probably close to the Benioff Zone, hence the
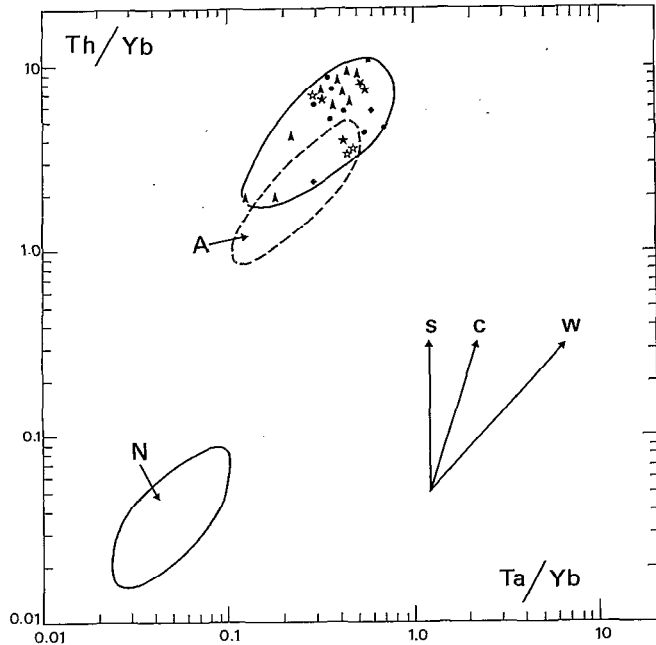
Fig. 14. — Th/Yb versus Ta/Yb diagram after PEARCE (1983), Table IX

s  subduction zone enrichment
c : crustal contamination
w : within plate enrichment
A : Central Andes, N-Tupe MORB
Symbols as in Fig. 7
arrow : data from JARAMILLO (1980) and MARRINER and MILLWARD (1984)

andesites with disequilibrium textures evidenced by multiple plagioclase, pyroxene and glass populations ;

3) Sr isotope ratios with very restricted ranges of values which indicate no significant increase with differentiation and the identical geochemical evolution through time suggest a common magmatic source ;

4) similar REE patterns with typical LREE enrichment for andesites and dacites from the 1985 eruption, and homogeneity of major mineral phases : plagioclase, orthopyroxene and clinopyroxene are also consistent with a single magmatic source ; but during the total history of Ruiz, small changes in the rate of fusion appear to have taken place ;

5) trace element compositions plotted in spidergrams show similar profiles for all the units and indicate only minor evolution through the last one Ma ;

6) minor and trace element data show LIL element enrichments related to the subduction zone source. The variability of the Th/Ta ratio (19 - 25 against 7 - 15) suggests the bimodality of the Ruiz products from a common source with a Th/Ta ratio near 5. The positive Ce anomaly and minor HFS element anomalies are due to an incompatible element enriched source from the subcontinental lithosphere ;

7) the similarity between the northern Colombian and Ecuadorian volcanic sources indicates that possible components considered for the origin of magma are subduction and within plate components with a probable small sialic crustal component.

subduction component in the source. This magma rises quickly, related to the intense activity of the major strike slip-faulting within the region (a mechanism of emplacement already invoked for granitic rocks (HUTTON, 1982) ) reaching a mid to high level chamber at some kilometers depth. This then supplies a shallow magma chamber beneath the active crater, as in the case of other volcanoes of this type in similar seetings e.g. Poás volcano in Costa Rica (THORPE et al., 1981 ; RYMER and BROWN, 1984).

## CONCLUSIONS

The knowledge of the structural setting, the stratigraphy of the main units and the petrochemical data of the Ruiz lavas lead us to following conclusions :

1) since Pliocene times, the petrogenesis of the products of the pyroclastic piedmont formations and the overlapping compound volcano activity at the intersection of two main structures originating in the Palaeozoic basement : the Palestina fault system (N20-30º) and the regional fault system (N120-130º) ;

2) lavas and pyroclastic flows are restricted to a narrow compositional range : 40 % dacites and 60 %

## TABLES I to XI

Table I
Representative microprobe analyses of plagioclase

| Ref: | 1 | 2 | 3 | 4 | 5 | 6 | 7 | 8 |
|------|-----|-----|-----|-----|-----|-----|-----|-----|
| SiO2 | 56,71 | 60,45 | 57,26 | 53,65 | 58,85 | 58,43 | 56,43 | 57,54 |
| Al2O3 | 28,51 | 25,78 | 26,55 | 29,34 | 26,19 | 26,34 | 26,35 | 26,21 |
| FeO* | 0,42 | 0,24 | 0,61 | 0,61 | 0,31 | 0,44 | 0,56 | 0,33 |
| CaO | 9,23 | 6,13 | 8,81 | 11,82 | 7,61 | 8,04 | 8,95 | 8,61 |
| Na2O | 4,39 | 6,73 | 6,01 | 4,34 | 5,98 | 6,16 | 5,86 | 6,11 |
| K2O | 0,37 | 0,69 | 0,64 | 0,32 | 0,71 | 0,73 | 0,75 | 0,58 |
| Total | 99,63 | 100,01 | 99,88 | 100,08 | 99,65 | 100,14 | 98,9 | 99,38 |
| AB% | 45,12 | 63,64 | 53,17 | 39,16 | 56,16 | 55,58 | 51,86 | 54,35 |
| OR% | 2,48 | 4,32 | 3,75 | 1,93 | 4,38 | 4,31 | 4,35 | 3,41 |
| AN% | 52,41 | 32,04 | 43,08 | 58,92 | 39,46 | 40,11 | 43,79 | 42,24 |

| | 9 | 10 | 11 | 12 | 13 | 14 | 15 | 16 |
|------|-----|-----|-----|-----|-----|-----|-----|-----|
| SiO2 | 58,64 | 54,41 | 58,99 | 55,04 | 57,41 | 57,33 | 57,84 | 53,59 |
| Al2O3 | 25,45 | 28,12 | 26,48 | 28,69 | 26,54 | 26,05 | 26,69 | 29,21 |
| FeO* | 0,41 | 0,47 | 0,35 | 0,45 | 0,38 | 0,44 | 0,37 | 0,48 |
| CaO | 8,02 | 10,94 | 7,51 | 10,82 | 8,04 | 7,72 | 8,52 | 11,15 |
| Na2O | 6,36 | 4,83 | 6,89 | 4,53 | 6,24 | 6,64 | 6,07 | 4,53 |
| K2O | 0,73 | 0,36 | 0,59 | 0,36 | 0,72 | 0,64 | 0,72 | 0,31 |
| Total | 99,61 | 99,13 | 100,81 | 99,89 | 99,33 | 98,82 | 100,21 | 99,27 |
| AB% | 56,43 | 43,45 | 60,34 | 42,15 | 55,92 | 58,65 | 53,96 | 41,56 |
| OR% | 4,25 | 2,11 | 3,32 | 2,18 | 4,27 | 3,71 | 4,18 | 1,87 |
| AN% | 39,32 | 54,44 | 36,34 | 55,67 | 39,81 | 37,64 | 41,86 | 56,58 |

| | 17 | 18 | 19 | 20 | 21 | 22 | 23 | 24 |
|------|-----|-----|-----|-----|-----|-----|-----|-----|
| SiO2 | 58,34 | 57,34 | 53,57 | 54,91 | 59,55 | 53,25 | 58,83 | 56,62 |
| Al2O3 | 26,48 | 25,81 | 28,58 | 28,02 | 25,78 | 28,96 | 25,61 | 27,97 |
| FeO* | 0,61 | 0,37 | 0,66 | 0,39 | 0,46 | 0,44 | 0,31 | 0,28 |
| CaO | 8,75 | 8,56 | 11,53 | 10,39 | 8,04 | 11,97 | 6,98 | 9,78 |
| Na2O | 5,89 | 6,33 | 4,49 | 5,13 | 5,45 | 4,26 | 6,46 | 5,26 |
| K2O | 0,54 | 1,01 | 0,32 | 0,38 | 0,86 | 0,38 | 1,04 | 0,51 |
| Total | 100,61 | 99,42 | 99,15 | 99,22 | 100,14 | 99,26 | 99,23 | 100,42 |
| AB% | 53,16 | 54,01 | 40,59 | 46,13 | 52,09 | 38,31 | 58,71 | 47,86 |
| OR% | 3,22 | 5,58 | 1,89 | 2,23 | 5,39 | 2,18 | 6,18 | 3,01 |
| AN% | 43,62 | 40,41 | 57,52 | 51,64 | 42,52 | 59,51 | 35,11 | 49,14 |

| | 25 | 26 | 27 | 28 | 29 | 30 | 31 | 32 |
|------|-----|-----|-----|-----|-----|-----|-----|-----|
| SiO2 | 54,73 | 55,79 | 55,07 | 57,48 | 56,79 | 54,01 | 58,54 | 54,91 |
| Al2O3 | 28,51 | 27,24 | 27,45 | 26,25 | 26,89 | 27,88 | 26,47 | 29,58 |
| FeO* | 0,53 | 0,56 | 0,38 | 0,34 | 0,39 | 0,67 | 0,01 | 0,41 |
| CaO | 10,61 | 9,75 | 9,71 | 8,64 | 8,73 | 10,16 | 7,74 | 10,21 |
| Na2O | 5,12 | 5,58 | 5,51 | 4,86 | 6,06 | 5,38 | 6,56 | 4,87 |
| K2O | 0,37 | 0,43 | 0,45 | 0,44 | 0,62 | 0,38 | 0,55 | 0,31 |
| Total | 99,87 | 99,35 | 98,57 | 98,01 | 99,48 | 98,48 | 99,87 | 100,29 |
| AB% | 45,63 | 49,57 | 49,35 | 49,03 | 53,65 | 47,82 | 58,56 | 45,45 |
| OR% | 2,16 | 2,51 | 2,62 | 2,88 | 3,63 | 2,24 | 3,23 | 1,92 |
| AN% | 52,21 | 47,92 | 48,03 | 48,09 | 42,72 | 49,94 | 38,21 | 52,64 |

| | 33 | 34 | 35 | 36 | 37 | 38 | 39 | 40 |
|------|-----|-----|-----|-----|-----|-----|-----|-----|
| SiO2 | 52,35 | 57,54 | 54,92 | 57,41 | 56,74 | 58,83 | 56,12 | 59,25 |
| Al2O3 | 28,28 | 26,52 | 28,28 | 25,06 | 26,81 | 25,86 | 27,51 | 25,84 |
| FeO* | 0,42 | 0,49 | 0,82 | 0,45 | 0,51 | 0,32 | 0,35 | 0,49 |
| CaO | 11,62 | 8,72 | 10,16 | 8,17 | 8,58 | 7,61 | 8,71 | 7,71 |
| Na2O | 4,32 | 5,93 | 5,29 | 6,09 | 6,08 | 6,46 | 5,94 | 6,31 |
| K2O | 0,33 | 0,49 | 0,41 | 0,71 | 0,59 | 0,58 | 0,43 | 0,77 |
| Total | 97,91 | 99,69 | 99,88 | 99,89 | 99,31 | 99,66 | 99,06 | 100,37 |
| AB% | 39,41 | 53,56 | 47,39 | 55,02 | 54,22 | 58,51 | 53,84 | 56,94 |
| OR% | 1,98 | 2,92 | 2,37 | 4,25 | 3,49 | 3,47 | 2,57 | 4,57 |
| AN% | 58,61 | 43,52 | 50,24 | 40,75 | 42,28 | 38,02 | 43,59 | 38,49 |

| | 41 | 42 | 43 | 44 | 45 | 46 | 47 | 48 |
|------|-----|-----|-----|-----|-----|-----|-----|-----|
| SiO2 | 58,55 | 57,94 | 59,43 | 57,83 | 55,72 | 52,47 | 55,87 | 55,41 |
| Al2O3 | 26,06 | 26,46 | 26,57 | 26,36 | 26,49 | 30,37 | 27,91 | 28,03 |
| FeO* | 0,66 | 0,41 | 0,37 | 0,45 | 0,69 | 0,61 | 0,45 | 0,61 |
| CaO | 8,47 | 8,32 | 7,33 | 7,87 | 9,56 | 12,57 | 9,79 | 10,15 |
| Na2O | 4,56 | 6,21 | 5,74 | 6,05 | 5,51 | 4,34 | 5,39 | 5,36 |
| K2O | 1,31 | 0,67 | 0,57 | 0,55 | 0,41 | 0,25 | 0,41 | 0,42 |
| Total | 99,61 | 100,01 | 100,01 | 99,11 | 100,38 | 100,61 | 99,82 | 99,98 |
| AB% | 45,17 | 55,17 | 56,47 | 56,21 | 49,81 | 37,93 | 48,66 | 47,65 |
| OR% | 8,49 | 3,92 | 3,69 | 3,36 | 2,38 | 1,44 | 2,43 | 2,44 |
| AN% | 46,35 | 40,91 | 39,84 | 40,43 | 47,81 | 60,73 | 48,91 | 49,92 |

(c) core. (r) rim. (mic) microlite. (phen) : phenocryst
FeO* as FeO total

*1985 er*
Biotite dacites
HC52b : anal. 1 (c) - 2 (r). same phen ,
FC7 : anal 3 included in cpx . 4 (c). phen..
    5 (c) - 6 (r). same phen. 7 (mic),
HC41 anal 8 (c) - 9 (r). same phen
    10 (c) - 11 (r). same phen
Two-pyroxene andesites
FC4 · anal. 12. microphen . 13 (c) - 14 (r). same phen .
JN48 anal 15 (c) - 16 (r). same phen.. 17 (c). phen..,
HC42 anal 18 (c) - 19 (r). same phen..
    20 (c) - 21 (r). same phen.. 22. 23 (c). phen.

*Historic er* .
Amphibole andesites :
83-212 anal. 24. 25 (c). phen..
83-212a : anal. 26 (c) - 27 (r). same phen..
    28 (c) - 29 (r). same phen . 30 (c). phen
83-227 . anal 31 (c) - 32 (r). same phen.

*Holocene er.* ·
Biotite dacites
83-111a . anal. 33 (c) - 34 (r). same phen., 35 (mic).
84-27a anal. 36 (c) - 37 (r). same phen.
    38 (c) - 39 (r). same phen

*Upper Unit*
Two-pyroxene andesites
83-186 · anal. 40 to 42 (c). phen.

*Basal Unit* :
Two-pyroxene andesites
83-255 . anal. 43. 44 (c). phen.

*Piedmont formations*
Two-pyroxene andesites
83-273 . anal. 45. 46 (c). phen..
    47 (c) - 48 (r). same phen.
    49 (c) - 50 (dusty zone) - 51 (r). same phen..
    52. 53 (mic)

| | 49 | 50 | 51 | 52 | 53 |
|------|-----|-----|-----|-----|-----|
| SiO2 | 54,72 | 54,19 | 52,55 | 58,68 | 64,97 |
| Al2O3 | 28,29 | 29,02 | 28,87 | 26,12 | 22,11 |
| FeO* | 0,52 | 0,55 | 0;57 | 0,71 | 0,51 |
| CaO | 10,55 | 10,82 | 11,29 | 8,28 | 3,65 |
| Na2O | 5,18 | 4,97 | 5,03 | 6,69 | 7,34 |
| K2O | 0,32 | 0,38 | 0,35 | 0,43 | 1,39 |
| Total | 99,58 | 99,93 | 98,66 | 100,91 | 99,97 |
| AB% | 46,14 | 44,38 | 43,73 | 57,91 | 71,44 |
| OR% | 1,91 | 2,21 | 2,01 | 2,47 | 8,87 |
| AN% | 51,95 | 53,41 | 54,27 | 39,62 | 19,69 |

Table II (A)
*Representative microprobe analyses of clinopyroxene*

| N ordre | 1 | 2 | 3 | 4 | 5 | 6 | 7 . |
|---|---|---|---|---|---|---|---|
| SiO2 | 52,71 | 52,95 | 53,62 | 52,48 | 50,04 | 53,56 | 53,22 |
| TiO2 | 0,46 | 0,17 | 0,32 | 0,48 | 1,04 | 0,23 | 0,19 |
| Al2O3 | 1,92 | 0,79 | 0,78 | 1,66 | 4,22 | 1,65 | 1,21 |
| FeO* | 8,94 | 8,71 | 7,72 | 9,65 | 9,24 | 9,29 | 17,36 |
| MnO | 0,42 | 0,51 | 0,37 | 0,29 | 0,16 | 0,17 | 0,51 |
| MgO | 14,34 | 13,84 | 15,15 | 14,44 | 14,82 | 14,49 | 22,66 |
| CaO | 20,01 | 22,01 | 22,36 | 20,54 | 20,06 | 20,73 | 4,61 |
| Na2O | 0,59 | 0,43 | 0,38 | 0,46 | 0,44 | 0,47 | 0,16 |
| Total | 99,38 | 99,41 | 100,71 | 100,01 | 100,02 | 100,58 | 99,91 |
| WO | 42,34 | 45,41 | 44,94 | 42,46 | 41,78 | 42,89 | 9,19 |
| EN | 42,19 | 39,74 | 42,35 | 41,49 | 42,94 | 41,69 | 62,89 |
| FS | 15,47 | 14,85 | 12,71 | 16,05 | 15,28 | 15,32 | 27,92 |
| Mg* | 61,59 | 61,37 | 66,24 | 59,94 | 61,59 | 73,11 | 69,31 |

| | 8 | 9 | 10 | 11 | 12 | 13 | 14 |
|---|---|---|---|---|---|---|---|
| SiO2 | 52,85 | 52,23 | 53,16 | 51,02 | 53,08 | 50,28 | 51,01 |
| TiO2 | 0,39 | 0,28 | 0,46 | 0,79 | 0,29 | 0,95 | 0,87 |
| Al2O3 | 1,32 | 1,37 | 1,13 | 4,75 | 1,57 | 5,09 | 2,92 |
| FeO* | 8,05 | 9,24 | 8,73 | 6,33 | 9,29 | 7,53 | 9,11 |
| MnO | 0,34 | 0,25 | 0,18 | 0,19 | 0,27 | 0,15 | 0,34 |
| MgO | 15,06 | 14,31 | 15,02 | 16,63 | 14,56 | 15,01 | 15,69 |
| CaO | 20,63 | 21,14 | 20,48 | 19,18 | 21,06 | 20,61 | 19,21 |
| Na2O | 0,48 | 0,61 | 0,51 | 0,41 | 0,51 | 0,47 | 0,28 |
| Total | 99,11 | 99,41 | 99,67 | 99,69 | 100,63 | 100,09 | 99,42 |
| WO | 42,86 | 43,64 | 42,37 | 40,46 | 43,19 | 43,39 | 39,69 |
| EN | 43,53 | 41,07 | 43,24 | 48,79 | 41,49 | 44,02 | 45,12 |
| FS | 13,61 | 15,29 | 14,39 | 10,75 | 15,32 | 12,58 | 15,19 |
| Mg* | 65,16 | 60,75 | 63,24 | 72,43 | 73,11 | 77,69 | 74,81 |

| | 15 | 16 | 17 | 18 | 19 | 20 | 21 |
|---|---|---|---|---|---|---|---|
| SiO2 | 52,31 | 51,91 | 52,35 | 52,17 | 51,44 | 51,95 | 52,04 |
| TiO2 | 0,34 | 0,39 | 0,44 | 1,39 | 0,46 | 0,86 | 0,37 |
| Al2O3 | 1,67 | 1,48 | 1,33 | 1,46 | 3,69 | 2,56 | 2,51 |
| FeO* | 8,68 | 9,52 | 9,21 | 8,93 | 7,96 | 9,27 | 5,09 |
| MnO | 0,28 | 0,35 | 0,38 | 0,24 | 0,23 | 0,67 | 0,16 |
| MgO | 14,84 | 14,37 | 14,28 | 14,26 | 15,31 | 14,57 | 17,95 |
| CaO | 21,25 | 20,89 | 21,52 | 20,57 | 18,37 | 19,24 | 18,97 |
| Na2O | 0,39 | 0,49 | 0,43 | 0,49 | 0,54 | 0,44 | 0,45 |
| Total | 99,76 | 99,53 | 99,94 | 99,51 | 97,99 | 99,37 | 97,53 |
| WO | 43,47 | 43,11 | 44,03 | 43,25 | 39,88 | 40,69 | 39,48 |
| EN | 42,22 | 41,07 | 40,65 | 41,69 | 46,24 | 42,87 | 51,98 |
| FS | 14,31 | 15,82 | 15,32 | 15,06 | 13,88 | 16,44 | 8,54 |
| Mg* | 75,31 | 72,86 | 73,45 | 73,98 | 77,41 | 73,69 | 86,25 |

| | 22 | 23 | 24 | 25 | 26 | 27 | 28 |
|---|---|---|---|---|---|---|---|
| SiO2 | 52,55 | 51,91 | 52,75 | 51,14 | 52,54 | 52,23 | 52,71 |
| TiO2 | 0,24 | 0,28 | 0,29 | 0,91 | 0,21 | 0,21 | 0,45 |
| Al2O3 | 1,44 | 1,95 | 1,09 | 4,57 | 1,75 | 1,31 | 1,22 |
| FeO* | 9,52 | 9,43 | 8,41 | 8,18 | 6,14 | 9,08 | 8,48 |
| MnO | 0,14 | 0,21 | 0,27 | 0,11 | 0,14 | 0,29 | 0,23 |
| MgO | 14,39 | 14,09 | 15,15 | 16,34 | 19,28 | 14,54 | 14,75 |
| CaO | 20,79 | 20,68 | 19,77 | 18,12 | 17,74 | 21,61 | 21,83 |
| Na2O | 0,49 | 0,62 | 0,49 | 0,46 | 0,25 | 0,39 | 0,48 |
| Total | 99,56 | 99,18 | 98,23 | 99,81 | 98,06 | 99,76 | 100,14 |
| WO | 42,99 | 43,25 | 41,52 | 38,29 | 35,86 | 43,96 | 44,42 |
| EN | 41,42 | 41,01 | 44,24 | 48,03 | 54,23 | 41,15 | 41,74 |
| FS | 15,59 | 15,74 | 14,24 | 13,68 | 9,92 | 14,89 | 13,84 |
| Mg* | 72,95 | 72,71 | 76,19 | 78,05 | 84,81 | 74,05 | 75,59 |

| | 29 | 30 | 31 | 32 |
|---|---|---|---|---|
| SiO2 | 52,41 | 52,75 | 53,13 | 51,51 |
| TiO2 | 0,41 | 0,41 | 0,23 | 0,01 |
| Al2O3 | 1,55 | 1,66 | 2,01 | 2,01 |
| FeO* | 10,07 | 8,89 | 5,53 | 8,47 |
| MnO | 0,34 | 0,29 | 0,25 | 0,21 |
| MgO | 14,69 | 16,22 | 15,97 | 14,49 |
| CaO | 19,39 | 17,67 | 22,34 | 21,49 |
| Na2O | 0,56 | 0,29 | 0,48 | 0,01 |
| Total | 99,42 | 98,19 | 100,01 | 98,19 |
| WO | 40,44 | 37,26 | 45,52 | 44,38 |
| EN | 42,62 | 47,61 | 45,27 | 41,63 |
| FS | 16,94 | 15,13 | 9,21 | 13,99 |
| Mg* | 72,18 | 76,45 | 83,71 | 75,61 |

(c) . core, (r) : rim, (mic) . microlite, (phen) : phenocryst.
FeO* as FeO total
Mg* = 100 Mg / (Mg + Fet)

*1985 er. :*
HC52b   anal. 1 (c). phen.
FC7 . anal. 2 (c) - 3 (r). same phen .
        4 (c) - 5 (r). same phen.
HC41 : anal. 6, 7 (c). phen.
FC4 · anal. 8, 9 (c). phen
JN48 : anal. 10 (c). phen . 11 (glomerophyre).
HC42 . anal. 12 (c) - 13 (r). same phen . 14 (r). phen.

*Historic er. :*
83-212 : anal. 15, 16 (c). phen.,
83-212a   anal. 17, 18 (c). phen.,
83-227 : anal. 19 (agglomerate), 20 (mic).

*Holocene er :*
83-111a . anal. 21 to 23 (c) phen.
84-27a   anal. 24 (c). phen., 25, 26 (mic).

*Upper Unit :*
83-186 : anal. 27, 28 (c). phen

*Basal Unit :*
83-255 : anal. 29 (c). phen., 30 (mic).

*Piedmont formations*
83-273 . anal. 31, 32 (c). phen.

Table II (B)
Representative microprobe analyses of orthopyroxene

| N ordre | 1 | 2 | 3 | 4 | 5 | 6 | 7 |
|---|---|---|---|---|---|---|---|
| SiO2 | 53,18 | 53,66 | 53,88 | 53,21 | 54,69 | 53,95 | 54,32 |
| TiO2 | 0,21 | 0,19 | 0,23 | 0,26 | 0,19 | 0,21 | 0,15 |
| Al2O3 | 2,33 | 0,82 | 0,67 | 0,88 | 0,66 | 0,71 | 0,78 |
| FeO* | 14,94 | 19,21 | 17,26 | 19,36 | 15,48 | 18,71 | 19,34 |
| MnO | 0,25 | 0,36 | 0,79 | 0,55 | 0,58 | 0,58 | 0,48 |
| MgO | 26,95 | 24,52 | 24,97 | 24,82 | 27,76 | 24,59 | 24,59 |
| CaO | 1,36 | 1,05 | 1,06 | 0,95 | 1,14 | 1,04 | 0,97 |
| Na2O | 0,02 | 0,02 | 0,04 | 0,01 | 0,01 | 0,11 | 0,01 |
| Total | 99,24 | 99,91 | 99,01 | 100,04 | 100,23 | 99,79 | 100,64 |
| WO | 2,69 | 2,07 | 2,13 | 1,87 | 2,18 | 2,06 | 1,91 |
| EN | 73,93 | 67,62 | 69,59 | 67,67 | 73,85 | 68,01 | 67,48 |
| FS | 23,38 | 30,31 | 28,26 | 30,47 | 23,97 | 29,93 | 30,61 |
| Mg* | 58,38 | 56,07 | 59,13 | 56,18 | 64,19 | 56,79 | 55,97 |

| | 8 | 9 | 10 | 11 | 12 | 13 | 14 |
|---|---|---|---|---|---|---|---|
| SiO2 | 54,41 | 54,11 | 53,48 | 54,37 | 53,07 | 55,56 | 53,89 |
| TiO2 | 0,17 | 0,23 | 0,13 | 0,33 | 0,21 | 0,05 | 0,41 |
| Al2O3 | 0,71 | 1,11 | 0,71 | 2,21 | 0,68 | 1,21 | 1,63 |
| FeO* | 18,05 | 17,88 | 20,65 | 13,17 | 20,73 | 9,19 | 15,67 |
| MnO | 0,42 | 0,45 | 1,19 | 0,01 | 0,57 | 0,23 | 0,41 |
| MgO | 24,79 | 25,84 | 23,47 | 28,36 | 23,19 | 31,48 | 26,74 |
| CaO | 0,92 | 1,04 | 1,27 | 1,06 | 1,09 | 1,55 | 1,72 |
| Na2O | 0,01 | 0,01 | 0,01 | 0,03 | 0,01 | 0,01 | 0,01 |
| Total | 99,47 | 100,72 | 100,91 | 99,58 | 99,58 | 99,29 | 100,48 |
| WO | 1,79 | 2,02 | 2,48 | 2,09 | 2,19 | 2,89 | 3,29 |
| EN | 69,19 | 70,07 | 64,05 | 77,67 | 64,52 | 83,12 | 72,29 |
| FS | 28,92 | 27,91 | 33,47 | 20,24 | 33,29 | 13,99 | 24,42 |
| Mg* | 57,86 | 59,09 | 53,19 | 68,28 | 52,79 | 77,39 | 63,05 |

| | 15 | 16 | 17 | 18 | 19 | 20 | 21 |
|---|---|---|---|---|---|---|---|
| SiO2 | 54,07 | 52,89 | 53,01 | 55,11 | 54,49 | 53,99 | 53,37 |
| TiO2 | 0,23 | 0,31 | 0,13 | 0,06 | 0,22 | 0,13 | 0,25 |
| Al2O3 | 3,71 | 1,39 | 0,97 | 0,97 | 1,82 | 0,85 | 0,89 |
| FeO* | 12,34 | 18,76 | 18,69 | 18,26 | 14,91 | 18,66 | 18,94 |
| MnO | 0,27 | 0,41 | 0,62 | 0,44 | 0,33 | 0,45 | 0,57 |
| MgO | 27,75 | 24,56 | 23,47 | 25,11 | 27,91 | 24,48 | 23,62 |
| CaO | 1,78 | 1,47 | 1,14 | 1,19 | 1,01 | 1,13 | 1,61 |
| Na2O | 0,01 | 0,01 | 0,05 | 0,01 | 0,02 | 0,05 | 0,02 |
| Total | 100,17 | 99,49 | 98,08 | 101,14 | 100,81 | 99,74 | 99,27 |
| WO | 3,59 | 2,89 | 2,34 | 2,38 | 1,95 | 2,26 | 3,24 |
| EN | 76,79 | 67,54 | 66,81 | 68,83 | 75,04 | 67,96 | 66,11 |
| FS | 19,62 | 29,57 | 30,86 | 28,79 | 23,01 | 29,78 | 30,65 |
| Mg* | 69,22 | 56,69 | 55,68 | 57,89 | 65,18 | 56,74 | 55,49 |

| | 22 | 23 | 24 | 25 | 26 | 27 | 28 |
|---|---|---|---|---|---|---|---|
| SiO2 | 55,61 | 55,71 | 53,26 | 51,83 | 53,69 | 53,11 | 53,49 |
| TiO2 | 0,04 | 0,01 | 0,05 | 0,28 | 0,25 | 0,19 | 0,29 |
| Al2O3 | 1,07 | 1,71 | 1,16 | 0,41 | 0,82 | 0,85 | 0,91 |
| FeO* | 7,86 | 7,58 | 19,89 | 18,86 | 18,01 | 20,13 | 18,19 |
| MnO | 0,21 | 0,19 | 0,56 | 0,74 | 0,53 | 0,59 | 0,39 |
| MgO | 33,79 | 32,83 | 24,75 | 24,71 | 25,26 | 24,34 | 25,62 |
| CaO | 1,31 | 1,21 | 0,87 | 0,74 | 1,41 | 1,21 | 1,15 |
| Na2O | 0,06 | 0,07 | 0,01 | 0,02 | 0,03 | 0,03 | 0,06 |
| Total | 100,25 | 99,68 | 100,53 | 97,71 | 100,02 | 100,51 | 100,13 |
| WO | 2,39 | 2,27 | 1,71 | 1,46 | 2,76 | 2,35 | 2,24 |
| EN | 86,08 | 86,27 | 67,15 | 68,18 | 68,87 | 66,08 | 69,48 |
| FS | 11,53 | 11,47 | 31,14 | 30,36 | 28,37 | 31,58 | 28,28 |
| Mg* | 81,13 | 81,24 | 56,71 | 56,72 | 58,38 | 54,73 | 58,48 |

| | 29 | 30 | 31 | 32 | 33 | 34 |
|---|---|---|---|---|---|---|
| SiO2 | 53,77 | 56,71 | 56,04 | 54,52 | 54,33 | 54,09 |
| TiO2 | 0,01 | 0,47 | 1,19 | 0,14 | 1,34 | 0,44 |
| Al2O3 | 0,74 | 1,37 | 1,45 | 3,71 | 2,74 | 0,94 |
| FeO* | 20,61 | 6,62 | 7,68 | 9,18 | 10,79 | 18,41 |
| MnO | 0,58 | 0,09 | 0,22 | 0,12 | 0,24 | 0,39 |
| MgO | 23,94 | 33,67 | 32,35 | 30,28 | 29,53 | 25,18 |
| CaO | 1,07 | 1,21 | 1,01 | 1,49 | 1,07 | 1,47 |
| Na2O | 0,06 | 0,19 | 0,42 | 0,05 | 0,43 | 0,06 |
| Total | 100,77 | 101,03 | 100,91 | 100,16 | 100,88 | 101,22 |
| WO | 2,11 | 2,27 | 1,93 | 2,94 | 2,09 | 2,87 |
| EN | 65,41 | 87,89 | 86,25 | 82,79 | 80,92 | 68,45 |
| FS | 32,48 | 9,84 | 11,82 | 14,27 | 16,99 | 28,68 |
| Mg* | 53,74 | 83,57 | 80,81 | 76,73 | 73,24 | 57,76 |

(c) : core, (r) rim, (mic) · microlite, (phen) · phenocryst.
FeO* as FeO total
Mg* = 100 Mg / (Mg + Fe t)

*1935 er*
HC52b anal. 1 (microphen). 2 (c). phen.
FC7 anal 3 (r). phen. , 4 (c) - 5 (r). same phen. ,
          6 (glomerophyre).
HC41 : anal 7. 8 (c). phen
FC4 anal 9. 10 (c). phen.
JN48 anal 12 (c) - 13 (r). same phen ,
          14. 15 (c) phen

*Historic er* ·
83-212 . anal 16 (c). phen.
83-212a anal 17 (r). phen
83-227 · anal 18 (r). phen. ; 19 (agglomerate)

*Holocene er.* :
83-111a : anal 20 (c). phen 21 (mic)
84-27a anal 22 (c) - 23 (r). same phen
          24 (c) - 25 (r). same phen

*Upper Unit*
83-186 anal 26 (mic) ; 27 (c). phen

*Basal Unit* .
83-255 anal 28 (c). phen . 29 (mic).

*Piedmont formations*
83-273 · anal 30 to 34 (c). phen

Table III
Representative microprobe analyses of amphibole

| Ref | 1 | 2 | 3 | 4 | 5 | 6 | 7 |
|---|---|---|---|---|---|---|---|
| SiO2 | 46,78 | 46,16 | 42,54 | 42,33 | 42,54 | 42,77 | 42,82 |
| TiO2 | 2,29 | 2,25 | 2,19 | 2,71 | 2,19 | 3,03 | 2,78 |
| Al2O3 | 7,99 | 8,01 | 13,35 | 13,27 | 13,35 | 13,02 | 13,44 |
| FeO* | 11,19 | 10,98 | 9,53 | 10,31 | 9,53 | 10,83 | 9,49 |
| MnO | 0,04 | 0,08 | 0,01 | 0,16 | 0,01 | 0,15 | 0,03 |
| MgO | 14,99 | 15,61 | 15,91 | 14,96 | 15,91 | 14,59 | 15,72 |
| CaO | 10,99 | 11,47 | 10,96 | 9,99 | 10,96 | 11,22 | 11,01 |
| Na2O | 1,92 | 2,02 | 2,54 | 2,51 | 2,54 | 2,57 | 2,51 |
| K2O | 0,94 | 0,85 | 0,54 | 0,65 | 0,54 | 0,58 | 0,66 |
| Total | 97,13 | 97,41 | 97,57 | 96,89 | 97,57 | 98,76 | 98,49 |
| Si | 6,79 | 6,76 | 6,18 | 6,19 | 6,18 | 6,19 | 6,17 |
| Al(IV) | 1,21 | 1,24 | 1,82 | 1,81 | 1,82 | 1,81 | 1,83 |
| Al(VI) | 0,16 | 0,14 | 0,46 | 0,49 | 0,47 | 0,41 | 0,45 |
| Ti | 0,25 | 0,25 | 0,24 | 0,29 | 0,24 | 0,33 | 0,29 |
| Fet | 1,36 | 1,33 | 1,16 | 1,26 | 1,16 | 1,31 | 1,14 |
| Mn | 0,01 | 0,01 | 0,01 | 0,02 | 0,01 | 0,02 | 0,01 |
| Mg | 3,42 | 3,41 | 3,44 | 3,27 | 3,45 | 3,15 | 3,37 |
| Ca | 1,71 | 1,79 | 1,71 | 1,57 | 1,71 | 1,74 | 1,71 |
| Na | 0,54 | 0,57 | 0,72 | 0,71 | 0,71 | 0,72 | 0,69 |
| K | 0,17 | 0,16 | 0,11 | 0,12 | 0,11 | 0,11 | 0,12 |
| Mg* | 71,54 | 71,92 | 74,78 | 72,18 | 74,83 | 70,59 | 73,55 |

| | 8 | 9 | 10 | 11 | 12 | 13 | 14 |
|---|---|---|---|---|---|---|---|
| SiO2 | 41,82 | 43,01 | 39,92 | 41,17 | 42,09 | 43,06 | 43,87 |
| TiO2 | 2,51 | 1,84 | 2,65 | 2,72 | 2,46 | 2,76 | 2,37 |
| Al2O3 | 13,18 | 11,81 | 13,44 | 12,99 | 12,63 | 12,67 | 13,45 |
| FeO* | 10,16 | 8,71 | 10,95 | 9,55 | 9,84 | 11,93 | 9,57 |
| MnO | 0,09 | 0,16 | 0,12 | 0,12 | 0,03 | 0,08 | 0,01 |
| MgO | 15,39 | 16,16 | 13,98 | 14,85 | 15,35 | 14,41 | 16,01 |
| CaO | 10,81 | 10,49 | 11,06 | 11,06 | 10,45 | 10,25 | 10,32 |
| Na2O | 2,56 | 2,45 | 2,52 | 2,52 | 2,53 | 2,35 | 2,65 |
| K2O | 0,67 | 0,42 | 0,53 | 0,54 | 0,49 | 0,61 | 0,61 |
| Total | 97,19 | 95,05 | 95,17 | 95,52 | 95,87 | 98,12 | 98,86 |
| Si | 6,13 | 6,38 | 6,03 | 6,14 | 6,23 | 6,27 | 6,27 |
| Al(IV) | 1,87 | 1,62 | 1,97 | 1,86 | 1,77 | 1,73 | 1,73 |
| Al(VI) | 0,41 | 0,44 | 0,42 | 0,42 | 0,44 | 0,44 | 0,53 |
| Ti | 0,27 | 0,21 | 0,29 | 0,31 | 0,27 | 0,31 | 0,25 |
| Fet | 1,25 | 1,08 | 1,38 | 1,19 | 1,22 | 1,45 | 1,14 |
| Mn | 0,01 | 0,02 | 0,02 | 0,02 | 0,01 | 0,01 | 0,01 |
| Mg | 3,36 | 3,57 | 3,15 | 3,31 | 3,39 | 3,13 | 3,41 |
| Ca | 1,69 | 1,67 | 1,79 | 1,77 | 1,66 | 1,61 | 1,58 |
| Na | 0,73 | 0,71 | 0,71 | 0,73 | 0,73 | 0,66 | 0,73 |
| K | 0,12 | 0,08 | 0,11 | 0,11 | 0,09 | 0,11 | 0,11 |
| Mg* | 72,97 | 76,78 | 69,47 | 73,48 | 73,55 | 68,28 | 74,87 |

(c) : core, (r) : rim, (mic) : microlite, (phen) : phenocryst
formulae amphiboles were calculated assuming :
FeO* as FeO total (see ROBINSON et al., 1982 for a justification of this assumption).
Mg* = 100 Mg / (Mg + Fe t)
Analyses have been recast on an anhydrous basis of 23 oxygens.

1985 er :
HC41 : anal. 1 (c) - 2 (r), same phen.
FC4 : anal. 3, 4 (c), phen.
HC42 : anal. 5 (c) - 6 (r), same phen.

Historic er. :
8-212 : anal. 7, 8 (c), phen.
82-212a : anal. 9 to 11 (c), phen., 12 (mic)
83-227 : anal. 13, 14 (c), phen.

Table IV
Representative microprobe analyses of phlogopite

| N ordre | 1 | 2 | 3 | 4 | 5 | 6 | 7 |
|---|---|---|---|---|---|---|---|
| SiO2 | 38,95 | 37,26 | 38,55 | 39,13 | 38,42 | 37,85 | 38,23 |
| TiO2 | 5,31 | 5,35 | 5,24 | 4,64 | 5,52 | 5,02 | 5,23 |
| Al2O3 | 13,78 | 13,44 | 13,76 | 13,47 | 13,41 | 13,77 | 13,61 |
| FeO* | 12,48 | 13,15 | 12,77 | 11,51 | 12,81 | 12,11 | 11,68 |
| MnO | 0,01 | 0,15 | 0,16 | 0,06 | 0,17 | 0,11 | 0,11 |
| MgO | 17,15 | 16,23 | 16,84 | 17,86 | 15,91 | 16,31 | 16,86 |
| CaO | 0 | 0,04 | 0 | 0 | 0 | 0,08 | 0,05 |
| Na2O | 0,62 | 0,74 | 0,62 | 0,76 | 0,88 | 0,61 | 0,78 |
| K2O | 8,26 | 8,75 | 7,83 | 8,17 | 8,27 | 8,85 | 8,63 |
| Total | 96,56 | 95,11 | 95,77 | 95,59 | 95,39 | 94,71 | 95,18 |
| Si | 5,61 | 5,51 | 5,63 | 5,69 | 5,66 | 5,61 | 5,62 |
| Al(IV) | 2,34 | 2,34 | 2,37 | 2,31 | 2,34 | 2,39 | 2,34 |
| Al(VI) | 0 | 0 | 0 | 0 | 0 | 0,01 | 0 |
| Ti | 0,57 | 0,59 | 0,57 | 0,51 | 0,61 | 0,58 | 0,58 |
| Fet | 1,49 | 1,63 | 1,56 | 1,41 | 1,57 | 1,44 | 1,43 |
| Mn | 0 | 0,02 | 0,02 | 0,01 | 0,02 | 0,01 | 0,01 |
| Mg | 3,68 | 3,58 | 3,61 | 3,87 | 3,49 | 3,69 | 3,97 |
| Ca | 0 | 0,01 | 0 | 0 | 0 | 0,01 | 0,01 |
| Na | 0,17 | 0,21 | 0,17 | 0,21 | 0,25 | 0,22 | 0,16 |
| K | 1,52 | 1,65 | 1,46 | 1,52 | 1,55 | 1,62 | 1,47 |
| Mg* | 71,18 | 68,71 | 69,82 | 73,29 | 68,97 | 71,93 | 73,52 |
| Mg/Fet | 2,27 | 2,19 | 2,76 | 2,21 | 2,41 | 2,57 | 2,69 |

| | 8 | 9 | 10 |
|---|---|---|---|
| SiO2 | 37,86 | 38,88 | 40,01 |
| TiO2 | 4,07 | 3,97 | 4,67 |
| Al2O3 | 13,29 | 14,29 | 15,16 |
| FeO* | 11,83 | 11,99 | 12,43 |
| MnO | 0,13 | 0,11 | 0,02 |
| MgO | 17,85 | 17,28 | 15,76 |
| CaO | 0,02 | 0,11 | 0,22 |
| Na2O | 0,55 | 0,38 | 0,27 |
| K2O | 7,72 | 7,57 | 5,93 |
| Total | 93,32 | 94,58 | 94,47 |
| Si | 5,65 | 5,69 | 5,79 |
| Al(IV) | 2,34 | 2,31 | 2,21 |
| Al(VI) | 0 | 0,16 | 0,37 |
| Ti | 0,46 | 0,44 | 0,51 |
| Fet | 1,48 | 1,47 | 1,51 |
| Mn | 0,01 | 0,01 | 0,01 |
| Mg | 3,97 | 3,77 | 3,39 |
| Ca | 0,01 | 0,02 | 0,03 |
| Na | 0,16 | 0,11 | 0,08 |
| K | 1,47 | 1,41 | 1,09 |
| Mg* | 72,84 | 71,95 | 69,18 |
| Mg/Fet | 2,69 | 2,57 | 2,26 |

(c) . core, (r) rim. (mic) · microlite. (phen) · phenocryst
FeO* as FeO total
Mg* = 100 Mg / (Mg + Fet)

*1985 er*
HC52b : anal 1 (c). lath
FC7   anal 2 (c). phen
HC41   anal 3 (c) - 4 (r). same phen
HC42   anal. 5 (c). phen.

*Holocene er*
83-111a   anal. 6, 7 (c) phen
84-27a   anal. 8 (c) - 9 (r). same phen . 10 (mic)

Table V
Representative microprobe analyses of olivine

| N ordre | 1 | 2 | 3 |
|---|---|---|---|
| SiO2 | 40,75 | 40,85 | 40,46 |
| FeO* | 12,61 | 14,88 | 18,61 |
| MnO | 0,19 | 0,12 | 0,22 |
| MgO | 46,72 | 45,04 | 40,81 |
| CaO | 0,14 | 0,11 | 0,11 |
| Total | 100,41 | 100,99 | 100,19 |
| Mg* | 78,76 | 75,18 | 68,67 |
| Fo | 86,69 | 84,31 | 79,41 |

(c) . core. (r) rim, (phen) phenocryst
Mg* = 100 Mg / (Mg + Fet)

*1985 er*
HC42   anal 1, 2 (c). 3 (r). phen.

Table VI (A)
Representative microprobe analyses of titanomagnetite

| N ordre | 1 | 2 | 3 | 4 | 5 | 6 | 7 |
|---|---|---|---|---|---|---|---|
| TiO2 | 6,11 | 8,71 | 12,06 | 8,63 | 11,99 | 9,51 | 8,39 |
| Al2O3 | 1,55 | 2,42 | 1,73 | 2,12 | 2,97 | 3,84 | 3,78 |
| Fe2O3 | 56,22 | 50,91 | 43,97 | 50,63 | 44,28 | 48,48 | 49,95 |
| FeO | 33,83 | 35,68 | 37,47 | 35,22 | 36,94 | 34,74 | 32,83 |
| MnO | 0,55 | 0,29 | 0,55 | 0,39 | 0,38 | 0,33 | 0,29 |
| MgO | 1,78 | 2,48 | 2,65 | 2,35 | 3,61 | 3,67 | 3,98 |
| Total | 100,04 | 100,49 | 98,43 | 99,34 | 100,17 | 100,57 | 99,22 |
| Usp% | 17,85 | 25,49 | 35,43 | 25,42 | 35,13 | 28,17 | 25,15 |

| N ordre | 8 | 9 | 10 | 11 | 12 | 13 | 14 |
|---|---|---|---|---|---|---|---|
| TiO2 | 9,61 | 7,65 | 7,67 | 9,73 | 9,86 | 8,72 | 6,03 |
| Al2O3 | 2,94 | 2,74 | 2,68 | 3,06 | 2,89 | 2,62 | 1,35 |
| Fe2O3 | 48,44 | 51,87 | 51,53 | 46,99 | 47,79 | 50,41 | 56,24 |
| FeO | 36,11 | 34,81 | 33,79 | 34,98 | 36,16 | 35,19 | 34,12 |
| MnO | 0,26 | 0,19 | 0,37 | 0,38 | 0,39 | 0,36 | 0,42 |
| MgO | 2,79 | 2,36 | 2,63 | 3,17 | 2,65 | 2,72 | 1,52 |
| Total | 100,15 | 99,62 | 98,67 | 98,31 | 99,74 | 100,02 | 99,68 |
| Usp% | 28,39 | 22,78 | 22,94 | 29,28 | 29,21 | 25,71 | 17,66 |

(c) : core, (r) : rim, (mic) : microlite, (phen) : phenocryst.
Ulvöspinel (Usp) after Carmichael (1967)
$XFe_2TiO_4 = Ti / Ti + (Fe^3 / 2)$

*1985 er.*
HC52b : anal. 1, 2 (c), phen,
FC7 : anal. 3 (mic)
HC41 : anal. 4 (mic).
JN48 : anal. 5 (c), phen.
HC42 : anal 6 (c). phen. ; 7 (mic)

*Historic er. :*
83-212 : anal. 8, 9 (mic), phen.
83-212a : anal. 10 (included in cpx).
83-227 : anal 11 (c), phen.

*Holocene er. :*
83-111a : anal. 12 (mic).
84-27a : anal. 13 (c). phen., 14 (mic).

Table VI (B)
Representative microprobe analyses of ilmenite

| N ordre | 1 | 2 | 3 | 4 | 5 | 6 | 7 | 8 |
|---|---|---|---|---|---|---|---|---|
| TiO2 | 36,09 | 29,61 | 28,92 | 39,87 | 33,42 | 29,15 | 30,47 | 34,49 |
| Al2O3 | 0,32 | 0,45 | 0,45 | 0,36 | 0,46 | 0,75 | 0,91 | 0,37 |
| Fe2O3 | 31,51 | 44,91 | 42,65 | 24,86 | 36,95 | 44,22 | 42,19 | 36,12 |
| FeO | 27,41 | 21,64 | 23,41 | 29,62 | 25,07 | 23,68 | 24,24 | 26,41 |
| MnO | 0,31 | 0,19 | 0,81 | 0,46 | 0,38 | 0,15 | 0,12 | 0,21 |
| MgO | 2,85 | 2,88 | 1,63 | 3,39 | 2,76 | 1,72 | 2,19 | 2,61 |
| Total | 98,45 | 99,68 | 97,87 | 98,56 | 99,04 | 99,67 | 100,12 | 100,21 |
| He% | 30,39 | 43,13 | 42,44 | 23,76 | 35,59 | 43,13 | 40,91 | 34,38 |

| N ordre | 9 | 10 | 11 | 12 | 13 | 14 | 15 | 16 |
|---|---|---|---|---|---|---|---|---|
| TiO2 | 33,91 | 36,36 | 31,41 | 32,63 | 35,77 | 27,84 | 33,63 | 48,94 |
| Al2O3 | 0,81 | 0,37 | 0,01 | 0,55 | 0,47 | 0,44 | 0,48 | 0,05 |
| Fe2O3 | 35,61 | 30,99 | 39,67 | 37,95 | 31,25 | 42,24 | 36,97 | 7,15 |
| FeO | 25,75 | 28,13 | 25,55 | 25,31 | 27,65 | 21,21 | 26,05 | 41,87 |
| MnO | 0,13 | 0,22 | 0,22 | 0,25 | 0,26 | 0,39 | 0,17 | 0,54 |
| MgO | 3,03 | 2,58 | 1,56 | 2,34 | 2,57 | 2,13 | 2,47 | 0,97 |
| Total | 99,24 | 98,65 | 98,42 | 99,03 | 97,97 | 94,25 | 99,77 | 99,52 |
| He% | 34,43 | 29,88 | 38,71 | 36,77 | 30,39 | 43,14 | 35,47 | 6,81 |

(c) : core, (r) : rim, (mic) : microlite, (phen) : phenocryst.
Hematite (He) after Carmichael (1967)
$XFe_2O_3 = (Fe^3 / 2) / (Fe^3 / 2) + Ti$

*1985 er. :*
HC52b : anal. 1 (small grain)
FC7 : anal. 2 (included in cpx). 3 (in plag.), 4 (in opx).
HC41 : anal. 5 (c), phen.
FC4 : anal. 6. 7 (c). phen.
HC42 : anal 8 (c) phen.

*Historic er. :*
83-212 : anal. 9 (mic)
83-212a : anal. 10, 11 (included in cpx).

*Holocene er. :*
83-111a : anal. 12 (c). phen. : 13 (small grain).

*Upper Unit :*
83-186 : anal. 14 (c). phen.

*Basal Unit. :*
83-255 : anal. 15 (in aggregates with cpx).

*Piedmont formations :*
83-273 : anal. 16 (phen).

Table VII
Representative microprobe analyses of glass and matrix

| N ordre | 1 | 2 | 3 | 4 | 5 | 6 | 7 | 8 |
|---|---|---|---|---|---|---|---|---|
| SiO2 | 74,51 | 71,72 | 74,07 | 74,99 | 75,05 | 67,96 | 64,86 | 63,75 |
| A1203 | 13,89 | 14,46 | 13,53 | 13,35 | 13,28 | 16,18 | 16,65 | 16,74 |
| FeO* | 1,34 | 1,72 | 1,48 | 1,23 | 1,19 | 2,98 | 4,06 | 4,39 |
| MnO | 0,04 | 0,07 | 0,01 | 0,12 | 0,09 | 0,07 | 0,13 | 0,12 |
| MgO | 0,19 | 0,42 | 0,26 | 0,23 | 0,27 | 0,99 | 1,63 | 1,79 |
| CaO | 1,04 | 1,46 | 0,95 | 0,89 | 0,88 | 2,53 | 4,05 | 4,39 |
| Na2O | 2,48 | 2,99 | 3,41 | 3,45 | 3,41 | 3,05 | 2,97 | 4,09 |
| K2O | 4,35 | 5,29 | 5,31 | 4,94 | 5,33 | 4,16 | 3,16 | 3,22 |
| TiO2 | 0,47 | 0,56 | 0,33 | 0,41 | 0,38 | 0,69 | 0,97 | 0,84 |
| Total | 98,58 | 99,53 | 99,35 | 99,61 | 99,89 | 98,75 | 99,13 | 99,33 |
| QZ | 40,11 | 29,25 | 30,53 | 32,95 | 31,74 | 25,37 | 21,61 | 13,28 |
| OR | 25,71 | 31,26 | 31,32 | 29,19 | 31,51 | 24,58 | 18,67 | 19,03 |
| AB | 20,99 | 25,31 | 28,86 | 29,19 | 28,86 | 25,81 | 25,13 | 34,61 |
| AN | 5,16 | 7,24 | 4,71 | 4,42 | 4,37 | 12,55 | 20,09 | 17,81 |
| CO | 3,21 | 1,16 | 0,46 | 0,71 | 0,31 | 2,06 | 0,98 | 0 |
| ILM | 0,89 | 1,06 | 0,63 | 0,76 | 0,72 | 1,31 | 1,84 | 1,61 |
| EN | 0,51 | 1,05 | 0,65 | 0,57 | 0,67 | 2,47 | 4,06 | 4,46 |
| FS | 1,76 | 2,36 | 2,19 | 1,81 | 1,74 | 4,46 | 6,11 | 5,91 |

| | 9 | 10 | 11 | 12 | 13 | 14 | 15 | 16 |
|---|---|---|---|---|---|---|---|---|
| SiO2 | 64,21 | 67,51 | 68,15 | 68,86 | 77,05 | 72,44 | 72,14 | 76,89 |
| A1203 | 17,04 | 16,44 | 15,82 | 15,58 | 12,81 | 14,68 | 14,51 | 13,26 |
| FeO* | 4,66 | 3,58 | 3,42 | 2,72 | 1,08 | 2,19 | 1,98 | 0,47 |
| MnO | 0,14 | 0,04 | 0,11 | 0,07 | 0,01 | 0,04 | 0,04 | 0,01 |
| MgO | 1,88 | 1,06 | 1,14 | 0,88 | 0,14 | 0,63 | 0,43 | 0,02 |
| CaO | 4,42 | 3,09 | 2,89 | 2,59 | 0,74 | 1,14 | 1,25 | 0,39 |
| Na2O | 3,94 | 2,11 | 2,74 | 2,73 | 2,22 | 1,87 | 2,32 | 2,42 |
| K2O | 3,24 | 3,55 | 3,78 | 3,71 | 4,95 | 5,79 | 3,56 | 7,15 |
| TiO2 | 0,82 | 0,78 | 0,98 | 0,63 | 0,25 | 0,78 | 0,62 | 0,25 |
| Total | 100,35 | 98,16 | 99,03 | 97,77 | 99,25 | 99,56 | 96,84 | 100,86 |
| QZ | 13,81 | 30,98 | 27,63 | 30,06 | 42,68 | 34,71 | 40,48 | 34,35 |
| OR | 19,15 | 20,98 | 22,34 | 21,92 | 29,25 | 34,27 | 21,04 | 42,25 |
| AB | 33,34 | 17,85 | 23,19 | 23,11 | 18,79 | 15,82 | 19,63 | 20,48 |
| AN | 19,24 | 15,38 | 14,39 | 12,85 | 3,67 | 5,66 | 6,21 | 1,98 |
| CO | 0 | 3,49 | 1,95 | 2,36 | 2,44 | 3,25 | 4,56 | 0,81 |
| ILM | 1,56 | 1,48 | 1,86 | 1,21 | 0,47 | 1,48 | 1,18 | 0,47 |
| EN | 4,68 | 2,64 | 2,84 | 2,19 | 0,35 | 1,57 | 1,07 | 0,05 |
| FS | 7,47 | 5,36 | 4,85 | 4,08 | 1,59 | 2,81 | 2,69 | 0,47 |

(w.ves) wall of vesicle. (gd) groundmass : (mt) matrix

*1985 er*
HC52b · anal. 1 (w ves)
FC7 anal 2 (w ves).
HC41 anal 3 to 5 (mt)
FC4 anal 6 (mt)
JN48 anal 7 (w ves)
HC42 . anal 8. 9 (mt)

*Historic er*
83-212 anal 10 (w.ves). 11 (mt)
83-212a anal 12 (mt)

*Holocene er*
84-27a anal 13 (w.ves)

*Upper Unit :*
83-186 anal 14 (gd)

*Basal Unit :*
83-255 anal. 15 (in aggregates with cpx)

*Piedmont formations*
83-273 anal 16 (mt)

Table VIII
Major element analyses and normative values of some representative whole-rock samples from the Nevado del Ruiz volcano and the Pliocene volcanic piedmont formations (sample localities in Appendix)

| N ordre | 1 | 2 | 3 | 4 | 5 | 6 | 7 | 8 |
|---|---|---|---|---|---|---|---|---|
| Ref | 83-273 | 83-267 | 82-85 | 83278a | 82-87 | 82-89 | 82-54 | 82-91 |
| SiO2 | 59,99 | 60,56 | 62,12 | 59,16 | 61,02 | 64,63 | 56,66 | 57,94 |
| Al2O3 | 15,03 | 15,07 | 17,02 | 16,87 | 16,69 | 17,93 | 17,36 | 17,21 |
| Fe2O3* | 5,81 | 5,44 | 5,08 | 5,81 | 5,44 | 3,61 | 7,42 | 6,07 |
| MgO | 5,14 | 6,15 | 4,23 | 3,66 | 5,01 | 2,51 | 4,78 | 5,97 |
| CaO | 6,09 | 5,74 | 5,47 | 5,52 | 5,29 | 5,49 | 7,13 | 5,92 |
| Na2O | 3,88 | 4,05 | 3,37 | 4,11 | 3,16 | 2,91 | 3,72 | 3,12 |
| K2O | 1,63 | 1,45 | 1,21 | 1,94 | 1,05 | 1,09 | 1,54 | 1,04 |
| TiO2 | 0,75 | 0,67 | 0,59 | 0,88 | 0,59 | 0,42 | 0,89 | 0,61 |
| MnO | 0,09 | 0,09 | 0,07 | 0,08 | 0,08 | 0,07 | 0,14 | 0,09 |
| P2O5 | 0,16 | 0,17 | 0,19 | 0,29 | 0,21 | 0,17 | 0,24 | 0,27 |
| L.O.I. | 0,86 | 0,12 | 0,16 | 0,71 | 0,53 | 0,62 | 0,57 | 0,58 |
| Total | 99,43 | 99,51 | 99,51 | 99,03 | 99,07 | 99,45 | 100,45 | 99,02 |
| Qz | 13,14 | 12,32 | 20,41 | 13,61 | 20,34 | 28,52 | 9,03 | 14,91 |
| Or | 9,63 | 8,57 | 7,09 | 11,46 | 6,19 | 6,44 | 9,11 | 6,15 |
| Ab | 32,83 | 34,27 | 28,52 | 34,78 | 26,74 | 24,54 | 31,48 | 26,41 |
| An | 18,78 | 18,66 | 25,96 | 21,85 | 25,06 | 26,24 | 26,12 | 27,78 |
| Co | 0 | 0 | 0,66 | 0 | 1,17 | 2,36 | 0 | 0,77 |
| Ilm | 0,21 | 0,19 | 0,15 | 0,17 | 0,17 | 0,15 | 0,31 | 0,19 |
| Hem | 5,81 | 5,44 | 5,08 | 5,81 | 5,44 | 3,61 | 7,42 | 6,07 |
| Ap | 0,38 | 0,41 | 0,47 | 0,71 | 0,51 | 0,41 | 0,57 | 0,64 |
| Ru | 0,64 | 0,57 | 0,52 | 0,79 | 0,49 | 0,34 | 0,74 | 0,71 |
| Di(Wo) | 4,38 | 3,68 | 0 | 2,96 | 0 | 0 | 3,27 | 0 |
| Di(En) | 3,79 | 3,18 | 0 | 2,09 | 0 | 0 | 2,03 | 0 |
| En | 9,02 | 12,14 | 10,54 | 7,72 | 12,45 | 6,25 | 9,08 | 14,87 |

| N ordre | 9 | 10 | 11 | 12 | 13 | 14 | 15 | 16 |
|---|---|---|---|---|---|---|---|---|
| Ref | 83-219 | 81-02 | 82-62 | 82-57 | 82-73 | 81-07 | 82-55 | 81-01 |
| SiO2 | 60,89 | 61,01 | 62,41 | 63,67 | 63,68 | 60,48 | 60,89 | 61,52 |
| Al2O3 | 16,07 | 15,56 | 15,45 | 18,51 | 17,78 | 15,63 | 16,27 | 16,33 |
| Fe2O3* | 5,54 | 6,14 | 5,01 | 4,03 | 4,21 | 7,07 | 4,82 | 5,68 |
| MgO | 5,19 | 4,27 | 3,12 | 1,71 | 2,74 | 5,07 | 4,35 | 3,49 |
| CaO | 5,43 | 5,15 | 5,04 | 4,97 | 4,18 | 5,56 | 4,92 | 4,61 |
| Na2O | 4,16 | 3,81 | 3,92 | 2,47 | 3,13 | 3,65 | 2,47 | 3,67 |
| K2O | 2,01 | 2,21 | 2,59 | 1,88 | 1,54 | 1,83 | 1,17 | 2,75 |
| TiO2 | 0,74 | 0,72 | 0,67 | 0,59 | 0,53 | 0,71 | 0,51 | 0,69 |
| MnO | 0,07 | 0,23 | 0,09 | 0,05 | 0,07 | 0,12 | 0,07 | 0,09 |
| P2O5 | 0,21 | 0,09 | 0,17 | 0,32 | 0,16 | 0,24 | 0,22 | 0,22 |
| L.O.I. | 0,67 | 0,83 | 0,89 | 1,41 | 0,96 | 0,03 | 3,19 | 0,77 |
| Total | 100,98 | 100,02 | 99,36 | 99,25 | 98,98 | 100,39 | 98,88 | 99,82 |
| Qz | 11,61 | 14,56 | 16,21 | 29,72 | 26,95 | 14,53 | 25,58 | 15,48 |
| Or | 11,82 | 13,06 | 15,31 | 11,11 | 9,11 | 10,81 | 6,91 | 16,25 |
| Ab | 35,19 | 32,24 | 33,17 | 20,91 | 26,49 | 30,89 | 20,91 | 31,06 |
| An | 19,27 | 18,83 | 16,91 | 22,77 | 19,81 | 20,86 | 23,11 | 19,96 |
| Co | 0 | 0 | 0 | 3,71 | 3,71 | 0 | 2,47 | 0 |
| Ilm | 0,15 | 0,49 | 0,19 | 0,11 | 0,15 | 0,26 | 0,15 | 0,19 |
| Hem | 5,54 | 6,14 | 5,01 | 4,03 | 4,21 | 7,07 | 4,82 | 5,68 |
| Ap | 0,51 | 0,24 | 0,41 | 0,76 | 0,38 | 0,57 | 0,52 | 0,52 |
| Ru | 0,66 | 0,46 | 0,57 | 0,53 | 0,45 | 0,57 | 0,42 | 0,59 |
| Di(Wo) | 2,69 | 2,56 | 2,96 | 0 | 0 | 2,22 | 0 | 0,67 |
| Di(En) | 2,32 | 2,21 | 2,56 | 0 | 0 | 1,92 | 0 | 0,58 |
| En | 10,61 | 8,42 | 5,21 | 4,26 | 6,83 | 10,71 | 10,84 | 8,11 |

| N ordre | 17 | 18 | 19 | 20 | 21 | 22 | 23 | 24 |
|---|---|---|---|---|---|---|---|---|
| Ref | 83-255 | 83-218 | 82-52 | 82-66 | 83-186 | 82-48 | 81-09 | 82-58 |
| SiO2 | 62,08 | 62,51 | 63,58 | 64,32 | 58,98 | 60,13 | 60,66 | 62,07 |
| Al2O3 | 15,77 | 15,63 | 16,59 | 18,25 | 15,95 | 15,62 | 16,47 | 16,58 |
| Fe2O3* | 4,72 | 4,79 | 4,73 | 3,76 | 4,49 | 5,93 | 6,15 | 5,18 |
| MgO | 3,29 | 3,96 | 3,84 | 2,04 | 4,49 | 4,51 | 4,36 | 3,77 |
| CaO | 4,72 | 4,61 | 4,97 | 5,13 | 6,01 | 5,66 | 5,36 | 5,29 |
| Na2O | 3,04 | 3,94 | 3,22 | 3,15 | 4,41 | 4,39 | 4,04 | 4,18 |
| K2O | 2,47 | 2,81 | 1,53 | 1,68 | 1,72 | 2,07 | 1,79 | 2,35 |
| TiO2 | 0,65 | 0,68 | 0,59 | 0,55 | 0,73 | 0,75 | 0,64 | 0,68 |
| MnO | 0,08 | 0,08 | 0,06 | 0,06 | 0,13 | 0,09 | 0,11 | 0,08 |
| P2O5 | 0,16 | 0,16 | 0,15 | 0,21 | 0,21 | 0,18 | 0,18 | 0,19 |
| L.O.I. | 2,14 | 0,81 | 0,23 | 0,56 | 0,68 | 0,25 | 0,21 | 0,45 |
| Total | 99,12 | 99,98 | 99,49 | 99,71 | 99,52 | 99,58 | 99,97 | 100,82 |

Table VIII (continued)

| N ordre | 17 | 18 | 19 | 20 | 21 | 22 | 23 | 24 |
|---|---|---|---|---|---|---|---|---|
| Ref | 83-255 | 83-218 | 82-52 | 82-66 | 83-186 | 82-48 | 81-09 | 82-58 |
| Qz | 20,42 | 14,61 | 29,01 | 28,07 | 9,86 | 10,44 | 13,65 | 12,51 |
| Or | 14,61 | 16,61 | 9,04 | 9,93 | 10,16 | 12,23 | 10,51 | 13,89 |
| Ab | 25,72 | 33,34 | 27,25 | 26,65 | 37,32 | 37,23 | 34,19 | 35,37 |
| An | 22,09 | 16,66 | 23,77 | 24,21 | 18,65 | 16,76 | 21,52 | 19,54 |
| Co | 0 | 0 | 0,92 | 2,38 | 0 | 0 | 0 | 0 |
| Ilm | 0,17 | 0,17 | 0,13 | 0,13 | 0,28 | 0,19 | 0,24 | 0,17 |
| Hem | 4,72 | 4,79 | 4,73 | 3,76 | 6,21 | 5,93 | 6,15 | 5,18 |
| Ap | 0,38 | 0,38 | 0,36 | 0,51 | 0,51 | 0,43 | 0,43 | 0,45 |
| Ru | 0,56 | 0,59 | 0,52 | 0,48 | 0,58 | 0,65 | 0,52 | 0,59 |
| Di(Wo) | 0,16 | 2,21 | 0 | 0 | 4,13 | 4,29 | 1,68 | 2,33 |
| Di(En) | 0,14 | 1,91 | 0 | 0 | 3,57 | 3,71 | 1,45 | 2,02 |
| En | 8,06 | 7,96 | 9,56 | 5,08 | 7,62 | 7,53 | 9,41 | 7,37 |

| N ordre | 25 | 26 | 27 | 28 | 29 | 30 | 31 | 32 |
|---|---|---|---|---|---|---|---|---|
| Ref : | 81-08 | 82-50 | 82-51b | 82-37 | 82-36 | 83-212 | 83-227 | 83-212a |
| SiO2 | 62,47 | 63,24 | 63,91 | 64,14 | 64,93 | 58,81 | 60,59 | 60,84 |
| Al2O3 | 15,64 | 17,72 | 18,31 | 18,91 | 16,79 | 16,11 | 15,53 | 15,51 |
| Fe2O3* | 5,58 | 4,61 | 3,28 | 3,02 | 4,11 | 5,55 | 5,56 | 5,58 |
| MgO | 4,29 | 3,76 | 2,49 | 1,91 | 3,12 | 5,76 | 3,78 | 4,14 |
| CaO | 4,52 | 4,57 | 3,61 | 5,18 | 4,03 | 5,97 | 5,87 | 6,11 |
| Na2O | 3,84 | 3,36 | 2,82 | 3,01 | 3,37 | 4,17 | 3,97 | 4,01 |
| K2O | 2,33 | 1,27 | 1,56 | 1,67 | 1,64 | 2,06 | 2,22 | 2,11 |
| TiO2 | 0,65 | 0,55 | 0,63 | 0,46 | 0,48 | 0,71 | 0,72 | 0,76 |
| MnO | 0,09 | 0,05 | 0,05 | 0,05 | 0,07 | 0,08 | 0,12 | 0,09 |
| P2O5 | 0,17 | 0,18 | 0,04 | 0,26 | 0,12 | 0,25 | 0,18 | 0,17 |
| L.O.I. | 0,31 | 0,51 | 2,48 | 0,82 | 0,45 | 0,35 | 0,92 | 0,11 |
| Total | 99,89 | 99,72 | 99,18 | 99,43 | 99,11 | 99,82 | 99,46 | 99,43 |
| Qz | 16,19 | 23,91 | 30,18 | 27,03 | 26,07 | 7,87 | 13,42 | 13,06 |
| Or | 13,77 | 7,51 | 9,22 | 9,87 | 9,69 | 12,17 | 13,12 | 12,41 |
| Ab | 32,49 | 28,43 | 23,86 | 25,39 | 28,52 | 35,29 | 33,59 | 33,93 |
| An | 18,56 | 21,61 | 17,67 | 24,17 | 19,29 | 19,13 | 18,01 | 18,12 |
| Co | 0 | 2,81 | 5,51 | 3,31 | 2,41 | 0 | 0 | 0 |
| Ilm | 0,19 | 0,11 | 0,11 | 0,11 | 0,15 | 0,17 | 0,26 | 0,21 |
| Hem | 5,58 | 4,61 | 3,28 | 3,02 | 4,11 | 5,55 | 5,56 | 5,58 |
| Ap | 0,41 | 0,43 | 0,09 | 0,62 | 0,28 | 0,59 | 0,43 | 0,41 |
| Ru | 0,55 | 0,49 | 0,57 | 0,41 | 0,41 | 0,62 | 0,58 | 0,65 |
| Di(Wo) | 1,21 | 0 | 0 | 0 | 0 | 3,77 | 4,21 | 4,67 |
| Di(En) | 1,03 | 0 | 0 | 0 | 0 | 3,25 | 3,63 | 4,04 |
| En | 9,65 | 9,37 | 6,23 | 4,73 | 7,77 | 11,09 | 5,78 | 6,27 |

| N ordre | 33 | 34 | 35 | 36 | 37 | 38 | 39 | 40 | 41 | 42 | 43 | 44 | 45 | 46 |
|---|---|---|---|---|---|---|---|---|---|---|---|---|---|---|
| Ref | ML-32a | HC-42 | ML-53 | ML-56 | HC-40 | ML-33 | 85-09 | FC-4 | ML-30 | FC-7 | JN-48 | HC52b | ML-41 | HC-41 |
| SiO2 | 60,01 | 60,21 | 60,51 | 60,55 | 60,71 | 61,11 | 61,25 | 61,27 | 61,81 | 62,41 | 62,51 | 63,66 | 63,71 | 64,51 |
| Al2O3 | 15,29 | 15,25 | 16,25 | 15,75 | 15,01 | 16,09 | 15,39 | 16,68 | 15,71 | 16,01 | 16,12 | 15,81 | 15,41 | 15,29 |
| Fe2O3* | 6,41 | 6,11 | 5,73 | 6,05 | 5,91 | 5,96 | 5,45 | 5,79 | 5,21 | 5,53 | 4,57 | 4,69 | 4,61 |
| MgO | 6,27 | 5,79 | 5,19 | 5,01 | 5,89 | 5,39 | 4,75 | 3,99 | 5,19 | 4,64 | 5,18 | 3,57 | 3,69 | 3,31 |
| CaO | 7,39 | 6,31 | 6,11 | 5,79 | 6,15 | 6,01 | 6,01 | 5,66 | 6,01 | 5,61 | 5,76 | 4,77 | 4,81 | 4,89 |
| Na2O | .3,61 | 3,65 | 3,79 | 3,65 | 3,65 | 3,69 | 3,65 | 3,28 | 3,59 | 2,25 | 2,04 | 3,51 | 3,59 | 3,89 |
| K2O | 2,01 | 2,11 | 2,15 | 2,15 | 2,09 | 2,01 | 2,11 | 1,89 | 2,01 | 1,94 | 1,88 | 2,24 | 2,59 | 3,01 |
| TiO2 | 0,69 | 0,75 | 0,71 | 0,69 | 0,75 | 0,69 | 0,75 | 0,69 | 0,75 | 0,64 | 0,67 | 0,61 | 0,71 | 0,55 |
| MnO | 0,09 | 0,09 | 0,09 | 0,09 | 0,09 | 0,09 | 0,09 | 0,09 | 0,09 | 0,11 | 0,11 | 0,08 | 0,07 | 0,08 |
| P2O5 | n.d. | n.d. | n.d. | n.d. | n.d. | n.d. | n.d. | 0,19 | n.d. | 0,22 | 0,22 | 0,17 | n.d. | n.d. |
| L.O.I. | 0,31 | 0,13 | 0,37 | 0,04 | 0,09 | 0 | 0,69 | 0,29 | 0 | 0,05 | 0,11 | 0,37 | 0,07 | 0,13 |
| Total | 101,08 | 100,38 | 100,89 | 99,28 | 100,48 | 100,99 | 100,65 | 99,49 | 100,93 | 99,09 | 100,12 | 99,34 | 99,34 | 100,27 |
| Qz | 10,95 | 11,43 | 11,36 | 13,78 | 12,09 | 12,82 | 14,28 | 17,74 | 14,54 | 23,52 | 23,94 | 20,02 | 18,23 | 16,84 |
| Or | 11,82 | 12,41 | 12,71 | 12,71 | 12,41 | 11,82 | 12,41 | 11,17 | 11,82 | 11,46 | 11,11 | 13,24 | 15,36 | 17,73 |
| Ab | 30,46 | 30,89 | 32,16 | 29,62 | 30,89 | 31,31 | 30,89 | 27,76 | 30,46 | 19,04 | 17,26 | 29,62 | 30,46 | 33,01 |
| An | 19,68 | 19,03 | 20,93 | 20,92 | 18,34 | 21,42 | 19,43 | 25,21 | 20,77 | 26,54 | 27,28 | 20,79 | 18,18 | 15,38 |
| Co | 0 | 0 | 0 | 0 | 0 | 0 | 0 | 0 | 0 | 0,48 | 0,73 | 0 | 0 | 0 |
| Ilm | 0,19 | 0,21 | 0,17 | 0,17 | 0,21 | 0,19 | 0,19 | 0,21 | 0,17 | 0,21 | 0,21 | 0,17 | 0,15 | 0,17 |
| Hem | 6,41 | 6,11 | 5,73 | 5,71 | 6,05 | 5,91 | 5,96 | 5,45 | 5,81 | 5,21 | 5,53 | 4,57 | 4,71 | 4,61 |
| Ap | 0 | 0 | 0 | 0 | 0 | 0 | 0 | 0,45 | 0 | 0,52 | 0,52 | 0,41 | 0 | 0 |
| Ru | 0,61 | 0,64 | 0,61 | 0,61 | 0,64 | 0,61 | 0,65 | 0,58 | 0,66 | 0,53 | 0,56 | 0,52 | 0,62 | 0,46 |
| Di(Wo) | 5,04 | 5,11 | 3,91 | 3,28 | 5,08 | 3,49 | 4,31 | 0,73 | 3,76 | 0 | 0 | 0,78 | 2,35 | 3,73 |
| Di(En) | 4,36 | 4,41 | 3,37 | 2,84 | 4,39 | 3,01 | 3,73 | 0,63 | 3,25 | 0 | 0 | 0,68 | 2,03 | 3,22 |
| En | 11,26 | 10,03 | 9,59 | 9,62 | 10,31 | 10,44 | 8,11 | 9,31 | 9,71 | 11,56 | 12,91 | 8,21 | 7,18 | 5,01 |

Table IX
Trace-element abundances for some representative lavas and pumices from the Nevado del Ruiz volcano and the Pliocene volcanic piedmont formations. Sample numbers correspond to samples listed in Table VIII (all values are in ppm ; n.a. not analysed)

| N ordre | 2 | 4 | 7 | 9 | 17 | 18 |
|---|---|---|---|---|---|---|
| Ref | 83-267 | 83-278a | 82-54 | 83-219 | 83-255 | 83-218 |
| La | 16,88 | 27,86 | 19,69 | 18,51 | 24,31 | 24,81 |
| Ce | 31,59 | 47,87 | 35,82 | 35,13 | 47,43 | 45,88 |
| Nd | 18,72 | 28,61 | 21,94 | 19,53 | 24,58 | 23,26 |
| Sm | 3,44 | 5,09 | 4,31 | 3,58 | 4,53 | 4,24 |
| Eu | 1,09 | 1,52 | 1,37 | 1,05 | 1,14 | 1,03 |
| Tb | 0,44 | 0,71 | 0,59 | 0,41 | 0,47 | 0,38 |
| Yb | 1,74 | 1,89 | 2,57 | 1,61 | 1,96 | 1,58 |
| Lu | 0,16 | 0,27 | 0,29 | 0,18 | 0,24 | 0,24 |
| U | 2,71 | 2,37 | 2,16 | 3,81 | 6,22 | 6,78 |
| Th | 5,31 | 6,93 | 6,02 | 9,36 | 12,98 | 16,65 |
| Hf | 3,22 | 3,71 | 2,58 | 3,29 | 4,19 | 4,16 |
| Sc | 15,63 | 16,91 | 24,26 | 13,98 | 13,19 | 12,09 |
| Cs | 1,31 | 2,01 | 4,25 | 4,73 | 3,61 | 9,13 |
| Ta | 0,81 | 0,93 | 0,74 | 0,97 | 0,55 | 1,09 |
| Zr | 118 | 129 | 86 | 120 | 137 | 151 |
| Ba | 937 | 1290 | 1346 | 1159 | 1248 | 1278 |
| Rb | 35 | 45 | 31 | 59 | 67 | 93 |
| Sr | 546 | 779 | 841 | 599 | 582 | 568 |
| Y | 16 | 22 | 21 | 17 | 16 | 17 |
| Nb | 2 | 6 | 3 | 5 | 5 | 8 |

| N ordre | 22 | 24 | 26 | 32 | 34 | 39 |
|---|---|---|---|---|---|---|
| Ref | 82-48 | 82-58 | 82-50 | 83-212a | HC-42 | 85-09 |
| La | 20,28 | 21,61 | 23,21 | 20,45 | 19,51 | 20,69 |
| Ce | 36,04 | 42,69 | 45,57 | 40,67 | 43,28 | 42,63 |
| Nd | 18,43 | 22,81 | 26,93 | 20,66 | 23,17 | 21,21 |
| Sm | 3,73 | 3,97 | 5,04 | 3,63 | 4,16 | 3,37 |
| Eu | 1,11 | 1,04 | 1,25 | 1,06 | 1,04 | 1,15 |
| Tb | 0,41 | 0,42 | 0,69 | 0,4 | 0,51 | 0,34 |
| Yb | 1,39 | 1,69 | 2,21 | 1,78 | 2,21 | 1,91 |
| Lu | 0,19 | 0,19 | 0,25 | 0,25 | 0,27 | 0,28 |
| U | 3,54 | 5,42 | 3,69 | 5,96 | 3,85 | 3,61 |
| Th | 10,13 | 13,05 | 8,79 | 10,75 | 11,31 | 10,81 |
| Hf | 3,45 | 4,08 | 3,46 | 3,82 | 3,72 | 3,89 |
| Sc | 15,11 | 13,65 | 14,89 | 16,73 | 22,31 | 15,12 |
| Cs | 7,18 | 8,52 | 5,84 | 2,95 | 2,38 | 2,24 |
| Ta | 0,92 | 1,04 | 0,96 | 0,46 | 0,81 | 0,68 |
| Zr | 133 | 131 | 123 | 120 | 102 | 122 |
| Ba | 1101 | 1184 | 850 | 1096 | 1792 | 1902 |
| Rb | 60 | 69 | 71 | 60 | 48 | 54 |
| Sr | 607 | 566 | 540 | 570 | 408 | 524 |
| Y | 15 | 13 | n.a. | 16 | 26 | 26 |
| Nb | 6 | 5 | n.a. | 5 | 4 | 6 |

| N ordre | 40 | 42 | 43 | 44 | 46 |
|---|---|---|---|---|---|
| Ref | FC-4 | FC-7 | JN-48 | HC-52b | HC-41 |
| La | 19,88 | 20,41 | 19,24 | 21,91 | 20,53 |
| Ce | 39,94 | 39,71 | 37,41 | 43,71 | 45,17 |
| Nd | 19,58 | 20,46 | 19,88 | 21,73 | 22,96 |
| Sm | 3,56 | 3,76 | 3,83 | 4,25 | 3,89 |
| Eu | 1,02 | 1,06 | 0,97 | 1,09 | 0,97 |
| Tb | 0,39 | 0,41 | 0,41 | 0,43 | 0,46 |
| Yb | 1,56 | 1,51 | 1,62 | 1,62 | 2,35 |
| Lu | 0,25 | 0,21 | 0,25 | 0,23 | 0,32 |
| U | 5,13 | 6,33 | 5,12 | 6,79 | 4,31 |
| Th | 10,39 | 11,32 | 10,28 | 14,11 | 13,96 |
| Hf | 3,73 | 3,72 | 3,68 | 4,51 | 4,22 |
| Sc | 16,63 | 16,94 | 17,63 | 14,49 | 20,59 |
| Cs | 2,91 | 3,06 | 2,73 | 3,96 | 2,91 |
| Ta | 0,53 | 0,71 | 0,49 | 0,56 | 1,07 |
| Zr | 123 | 220 | 120 | 149 | 136 |
| Ba | 1063 | 1162 | 943 | 1177 | 2210 |
| Rb | 54 | 65 | 62 | 78 | 72 |
| Sr | 563 | 570 | 544 | 494 | 440 |
| Y | 10 | n.a. | n.a. | 17 | 26 |
| Nb | 3 | n.a. | n.a. | 5 | 6 |

Table X
Trace element abundances for separate minerals and groundmas-
ses from two 1985 pumices

A:br.pum

| N ordre | 34-pl | 34-cpx | 34-opx | 34-mgt | 34-gm |
|---|---|---|---|---|---|
| Ref:HC42 | | | | | |
| La | 11,55 | 11,17 | 10,01 | 14,48 | 13,86 |
| Ce | 17,54 | 36,39 | 24,55 | 30,37 | 25,52 |
| Nd | 5,89 | 35,79 | 16,55 | 18,69 | 11,97 |
| Sm | 0,74 | 10,05 | 4,22 | 3,74 | 1,77 |
| Eu | 1,25 | 1,65 | 0,74 | 0,73 | 0,42 |
| Tb | 0,18 | 1,56 | 0,55 | 0,39 | 0,15 |
| Yb | 0,17 | 4,79 | 2,81 | 1,57 | 0,84 |
| Lu | 0,06 | 0,83 | 0,45 | 0,28 | 0,11 |
| U | 0,16 | n.a. | 0,56 | 2,33 | 6,01 |
| Th | 1,34 | 1,56 | 1,83 | 5,53 | 10,76 |
| Hf | 0,41 | 2,37 | 1,37 | 6,03 | 5,31 |
| Sc | 0,59 | 109 | 43 | 37 | 4,55 |
| Cs | 0,55 | n.a. | 0,58 | 1,97 | 2,91 |
| Ta | 0,15 | 0,51 | 0,21 | 2,26 | 0,96 |
| Zr | 47 | n.a. | 221 | 270 | 224 |

B:wh.pum

| N ordre | 46-pl | 46-cpx | 46-opx | 46-mgt | 46-gm |
|---|---|---|---|---|---|
| Ref:HC41 | | | | | |
| La | 13,13 | 18,67 | 19,42 | 30,67 | 18,14 |
| Ce | 19,14 | 51,55 | 46,16 | 69,85 | 34,88 |
| Nd | 6,61 | 42,15 | 31,93 | 43,99 | 17,73 |
| Sm | 0,79 | 12,74 | 7,04 | 8,31 | 2,72 |
| Eu | 1,46 | 1,89 | 1,01 | 0,91 | 0,67 |
| Tb | 0,15 | 1,73 | 0,91 | 0,83 | 0,21 |
| Yb | 0,13 | 5,83 | 3,64 | 2,31 | 1,14 |
| Lu | 0,03 | 0,84 | 0,58 | 0,36 | 0,16 |
| U | 0,18 | 0,31 | 0,46 | 3,03 | 6,49 |
| Th | 1,16 | 2,46 | 2,21 | 5,86 | 12,73 |
| Hf | 0,31 | 2,75 | 1,68 | 8,76 | 4,95 |
| Sc | 0,23 | 103 | 48 | 42 | 8 |
| Cs | 0,45 | 0,92 | 0,56 | 2,05 | 1,97 |
| Ta | 0,41 | 0,52 | 0,31 | 3,59 | 0,57 |
| Zr | 72 | 409 | 160 | 762 | 218 |

Sample numbers correspond to whole-rock samples listed in Table 8
A · anal 34 (HC42) andesitic brown pumice
B . anal 46 (HC41) dacitic white pumice
(all values are in ppm  n a   not analysed, below detection limit)
pl  plagioclase . cpx  clinopyroxene . opx : orthopyroxene . mgt · titanomagnetite . gm
groundmass
Olivine and biotite phenocrysts were not analysed

Table XI
Isotopic Sr compositions of some representative lavas of the
Nevado del Ruiz and the Pliocene volcanic piedmont formations.
Analyses performed by L BRIQUEU (Laboratoire de Géochimie Iso-
topique, Univ. Montpellier, France). Sample references correspond
to samples listed in Table VIII. (A : volcanic piedmont formations ;
b · Basal Unit : C · Upper Unit)

| Ref | 87Sr/86Sr | σ |
|---|---|---|
| A : | | |
| 83-267 | 0.704511 | 0.000035 |
| 83-278a | 0.704674 | 0.000048 |
| B : | | |
| 82-54 | 0.704022 | 0.000053 |
| 83-219 | 0.704275 | 0.000046 |
| 83-218 | 0.704480 | 0.000054 |
| C : | | |
| 82-48 | 0.704080 | 0.000045 |
| 82-58 | 0.704369 | 0.000055 |
| 82-50 | 0.704273 | 0.000053 |

## APPENDIX (cf. Table VIII)

Abbreviations : ol  olivine - cpx : clinopyroxene - opx . orthopyroxene - amph . amphibole
- bi : biotite - pl · plagioclase - aph  aphyric - porph · porphyritic - and : andesite - dac
dacite - pum  fall  pumice fall - ash fl. : ash flow - pum. fl. · pumice flow - pyrocl. fl. ·
pyroclastic flow - r. : rio - C : Cerro - qba  quebrada - Par. Nev · Parque de los Nevados
- weath. : weathered - 1985 er. : last eruption of the Nevado del Ruiz volcano.

MA : Microprobe Analyses : REE : Rare Earth Elements ,
AA · Atomic Absorption ; XRF . energy-dispersive X-Ray Fluorescence :
SIC   Strontium Isotopic Compositions.

Phosphorus was not analysed (n d) in samples n° 33 to 39 and 45. Fe2O3* as Fe2O3 total.
L.O.I. = Loss of ignition. oxides (wt%) by XRF or AA
— the Pliocene volcanic piedmont formations (anal. n° 1-6)
— the Basal Unit  the first episode (anal. n° 7-13)
            the last episode (anal. n° 14-20)
— the Upper Unit (anal. n° 21-29)
— the historic er. (anal. n° 30-32)
— the 1985 eruption (anal. n° 33-46)

```
 n    Ref      N latit.   W longit.  alt.(m)   rock name        location
---------------------------------------------------------------------------------

A- Piedmont formations

     Consota Fm., Cauca basin, W. Piedmont.

 1   83-273   4°43'05"   75°36'10"   2000    2px-and, lava fl.,
                                             Puerta Risaralda,
                                             r. Barbas, Pereira-Armenia
                                             road, !(XRF, MA)
 2   83-267   4°47'00"   75°53'00"   1150    amph-and, porph.lava fl.,
                                             Fonda Placer. r.Consota,
                                             (XRF, MA, REE, SIC)
 3   82-85    4°37'00"   75°45'30"   1250    and, block lava, Quimbaya,
                                             (XRF)

     Casabianca Fm., Magdalena valley, E. Piedmont.

 4   83278a   5°09'30"   75°02'00"   1550    and, pyrocl. flow, Fresno,
                                             upper Pliocene-Pleistocene,
                                             (XRF, REE. SIC)
 5   82-87    5°05'00"   75°10'45"   2200    and, pyroclastic fl.,
                                             Herveo, Pueblo Abajo,
                                             (XRF)
 6   82-89    5°04'50"   75°12'30"   1880    dac,lava flow, Herveo,
                                             (XRF)

B- Ruiz formations

     Basal unit I

 7   82-54    5°01'00"   75°22'00"   3250    2px-and,lava flow. Pena
                                             Margarita (1.05 Ma),
                                             (XRF, REE, SIC)
 8   82-91    5°02'00"   75°07'00"   1950    cpx-and,lava flow. Villa
                                             Hermosa, (XRF)
 9   83-219   4°58'00"   75°21'00"   3950    amph-and,lava flow,
                                             Alto Aquila, C.El Arbolito,
                                             (XRF, REE. SIC)
10   81-02    4°50'00"   75°14'00"   2900    2px-and,lava flow, r.Recio,
                                             (XRF)
11   82-62    5°02'00"   75°26'00"   2360    opx-and, lava fl.. Tesoro
                                             (1.2 Ma), (XRF)
12   82-57    4°59'00"   75°24'00"   3280    amph-dac, aph.lava flow,
                                             Termales -abajo, (XRF)
13   82-73    4°50'00"   75°12'50"   2450    amph-dac, lava flow,
                                             r.Recio. Esperanza. (XRF)

     Basal unit II

14   81-07    4°54'00"   75°15'30"   3500    cpx-and,lava flow. Murillo,
                                             La Cabana. (XRF)
15   82-55    5°00'30"   75°19'45"   3550    cpx-and,lava flow,
                                             Esperanza, Murillo road,
                                             (XRF)
16   81-01    4°55'00"   75°05'00"   1900    2px-and,lava flow, Libano,
                                             (XRF)
17   83-255   4°59'20"   75°32'45"   1600    2px-and, grey pum., ash flow,
                                             Miraflores,
                                             (XRF, MA, REE)
18   83-218   4°56'00"   75°17'30"   3600    amph-and, porph. Lava-dome,
                                             Pena Cachucha,
                                             (XRF, REE, SIC)
19   82-52    4°56'30"   75°21'00"   4000    opx-dac,lava flow, Murillo
                                             road, Guali headwaters,
                                             (XRF)
20   82-66    4°51'00"   75°16'00"   3220    amph-dac, porph.lava flow,
                                             El Oso, (XRF)
```

21  83-186  4°58'00"  75°33'00"  2000  2px-and, black scoria,
                                        ash fl.,Riobamba,
                                        La Oliva, (XRF)

22  82-48   4°53'00"  75°25'00"  3300  opx-and,lava flow, La Pica,
                                        r.Claro (0.20 Ma)
                                        (XRF, REE, SIC)

23  81-09   4°55'00"  75°16'00"  4000  cpx-porphy.and,dome,Alto
                                        La.Piramide, (XRF)

24  82-58   4°56'00"  75°28'00"  2250  2px porphy.and,block-lava,
                                        La Laguna,
                                        (XRF, REE, SIC)

25  81-08   4°53'00"  75°15'00"  3700  2px-porphy.and.lava flow,
                                        La Leonera Alta, (XRF)

26  82-50   4°54'00"  75°16'30"  4375  amph-porphy.dac,dome, Alto
                                        La Piramide,
                                        (XRF, REE, SIC)

27  82-51b  4°54'00"  75°16'30"  4350  amph-dac. weath.breccia,
                                        Alto La Piramide,
                                        (XRF)

28  82-37   4°52'45"  75°21'45"  4250  bi-dac.lava flow, near the
                                        Refugio, (XRF)

29  82-36   4°54'00"  75°21'00"  4650  opx-dac, porph. lava flow,
                                        Refugio. (XRF)

30  83-212  4°55'00"  75°18'05"  4150  amph-and, grey pum., pum. fl.,
                                        qda near the r. Azufrado,
                                        (XRF)

31  83-227  4°55'10"  75°18'10"  4100  and-grey pum. fl.,r. Azufrado,
                                        upper sequence
                                        (310 +/- 70 BP) (XRF, MA)

32  83-212a 4°55'00"  75°18'05"  4150  amph-and, white pum., pum. fl.,
                                        qda near the r. Azufrado,
                                        (XRF, MA, REE)

33  ML-32a  4°54'30"  75°18'00"  4400  and-black pum.,up. part of
                                        the pyrocl.flow. (AA)

34  HC-42   4°57'15"  75°21'10"  4100  2px-and, brown pum,
                                        last pum. fall, C.Guali,
                                        (AA, MA, REE)

35  ML-53   4°53'30"  75°17'15"  4600  brown pum., Lagunilla glacier,
                                        last pum. fall, (AA)

36  ML-56   4°54'30"  75°20'15"  4700  white pum., Guali headwaters,
                                        pum.fall on surge deposit,
                                        (AA)

37  HC-40   4°58'15"  75°21'00"  4000  2px-and., grey pum., last pum.
                                        fall, Termales de Ruiz,
                                        (AA)

38  ML-33   4°55'00"  75°18'00"  4400  and-black pum., pum.-rich lahar
                                        r. Azufrado, 1985 er. (AA)

39  85-09   4°53'50"  75°21'15"  4700  and-black pum.,pum.-rich lahar,
                                        near the Olleta crater,
                                        (XRF, REE)

40  FC-4    4°55'00"  75°21'30"  4270  and-black pum. pum.-rich lahar,
                                        N r. Molinos,
                                        (XRF, MA, REE)

41  ML-30   4°54'30"  75°18'30"  4400  grey pum., Azufrado headwaters,
                                        pum.fall betw. surge and
                                        pum.-rich lahar, (AA)

42  FC-7    4°54'55"  75°21'30"  4450  bi-dac. grey pum, N r.
                                        Molinos, near the Refugio,
                                        (XRF, MA, REE)

43  JN-48   4°53'40"  75°17'00"  3950  2px-and, brown pum.,
                                        r. Lagunilla,
                                        (XRF, MA, REE)

44  HC-52b  4°56'20"  75°19'10"  4120  2px, bi-dac.,white pum.,
                                        last pum. fall,  Murillo road,
                                        betw.queb.Lisa and Marcada,
                                        (XRF, MA, REE)

45  ML-41   4°56'00"  75°17'45"  3700  grey pum., Plan Plazuela
                                        Azufrado, last pum. fall,
                                        (AA)

46  HC-41   4°57'45"  75°21'30"  4020  bi-dac, white pum., last pum.
                                        fall, Par.Nev. road,
                                        (AA, MA, REE)

# BIBLIOGRAPHIE

ARCO (P. d'), 1982. — Contribution à l'interprétation géothermique et géobarométrique des paragénèses calco-alcalines de l'Arc des Petites Antilles ; cristallisation fractionnée de la série du Quill (Ile de Saint-Eustache). *Thèse Doct. Brest*, 186 p.

BOILY (M.), BROOKS (C.), JAMES (D.E.), 1983. — Geochemical characteristics of the last mesozoic andean volcanics. In « Andean Magmatism ». (Eds RS Harmon and Ba Barreiro) : 190-202. Shiva Pub. Cheshire, UK.

BRIQUEU·(L.), 1985. — Étude du magmatisme associé aux zones de subduction à l'aide de traceurs géochimiques multiples : éléments traces et rapports isotopiques [87] Sr / [86] Sr - [143] Nd / [144] Nd. *Doc. Trav. CGG, Montpellier*, 5, 154 p.

BRIQUEU (L.), BOUGAULT (H.), JORON (J.L.), 1984. — Quantification of Ta, Nb, Ti and V anomalies in magmas associated with subduction zones : petrogenetic implications. *Earth Planet. Sci. Lett.*, 68 : 297-308.

BRIQUEU (L.), JAVOY (M.), LANCELOT (J.R.), TATSUMOTO (M.), 1986. — Isotope geochemistry of recent magmatism in the Aegean arc : Sr, Nd, Hf, and O isotopic ratios in the lavas and Milos and Santorini. Geodynamic implications. *Earth Planet. Sci. Lett.*, 80 : 41-54.

BROWN (G.C.), RYMER (H.), THORPE (R.S.), 1987. — The evolution of andesite volcano structures : new evidence from gravity studies in Costa Rica. *Earth Planet Sci. Lett.*, 82 : 323-334.

BUDDINGTON (A.E.) and LINDSLEY (D.H.), 1964. — Iron-titanium oxide minerals and synthetic equivalents. *J. Petrol.*, 5 : 310-353.

CANTAGREL (J.M.), THOURET (J.C.), VATIN-PÉRIGNON (N.), SALINAS (R.), MURCIA (A.), 1986. — The Nevado del Ruiz : Quaternary to historic activity (abstr.). *Eos*, 16 : 405.

CARMICHAEL (I.S.E.), 1967. — The iron-titanium oxides of salic volcanic rocks and their associated ferromagnesian silicates. *Contrib. Mineral. Petrol.*, 14 : 36-64.

DOSTAL (J.), ZENTILLI (M.), CAELLES (J.), CLARK (A.H.), 1977. — Geochemistry and origin of volcanic rocks of the Andes (26°-28°S). *Contrib. Mineral. Petrol.*, 63 : 113-128.

FRANCIS (P.W.), MOORBATH (S.), THORPE (R.S.), 1977. — Strontium isotopes data for recent andesites in Ecuador and North Chile. *Earth Planet. Sci. Lett.*, 37 : 197-202.

GILL (J.B.), 1981. — Orogenic andesites and plate tectonics. Springer Verlag eds, Berlin, Heidelberg, New York, 390 p.

GOEMANS (P.), 1986. — *Pétrogéochimie du volcan Solimana, Sud Pérou. (Géochimie comparée de quelques édifices des Andes centrales et septentrionales).* Mém. DGUG. Univ. Grenoble, 114 p. (unpublished).

GOEMANS (P.), OLIVER (R.A.), VATIN-PÉRIGNON (N.), BRIQUEU (L.), DUPUY (C.). — Geochemical evolution of the Nevado Solimana, Western Cordillera, Southern Peru. *J. Geol. Soc. London* (submitted).

GOEMANS (P.), VATIN-PÉRIGNON (N.), OLIVER (R.A.), 1987a. — Geochemistry of dacitic lavas from Solimana volcano, Western Cordillera, Southern Peru (Abstr.). *Terra Cognita*, 7 : 2-3, 280-281.

GOEMANS·(P.), VATIN-PÉRIGNON (N.), OLIVER (R.A.), BRIQUEU (L.), 1987b. — Geochemistry of dacites and role of the continental crust in the genesis of the Solimana volcano, Western Cordillera, Southern Peru (extended abstr.). *Decimo Congreso geologico argentino*. Project 249, International symposium « Andean volcanism », 4 : 325-327.

HARMON (R.S.), BARREIRO (B.A.), MOORBATH (S.), HOEFS (J.), FRANCIS (P.W.), THORPE (R.S.), DERUELLE (B.), McHUGHS (J.),

VIGLINO (J.A.), 1984. — Regional O, Sr and Pb-isotope relationships in late Cenozoic calc-alkaline lavas of the Andean Cordillera. *J. Geol. Soc. London*, 141 : 803-822.

HAWKESWORTH (C.J.), HAMMILL (A.R.), GLEDHILL (A.R.), van CALSTEREN (P.), ROGERS (G.), 1982. — Isotope and trace element evidence for late-stage intra-crustal melting in the high Andes. *Earth Planet Sci. Lett.*, 58 : 240-254.

HELLER (E.), CARRACEDO (J.C.), SOLER (V.), 1986. — Reversed magnetization in pyroclastics from the 1985 eruption of Nevado del Ruiz, Colombia. *Nature*, 324 : 241-242.

HERD (D.G.), 1982. — Glacial and volcanic geology of the Ruiz-Tolima volcanic complex, Cordillera Central, Colombia. *Publ. geol. Espec. 8, Ingeominas, Bogotá*, 48 p.

HERD (D.G.), 1986. — The 1985 Ruiz volcano disaster. *Eos* May 13 : 457-460.

HUTTON (D.H.W.), 1982. — A tectonic model for the emplacement of the Main Donegal granite, NW Ireland. *J. Geol. Soc. London*, 139 : 615-630.

INGEOMINAS, 1976a. — Mapa geologico K8, Manizales, 1/1000.000. Informe preliminar inedito, por Mosquera D., CJ Vesga, R Marin, Bogotá.

INGEOMINAS, 1976b. — Mapa geologico de Colombia, 1/1'500.000. Compilación geologica J.L. Arango Cálad, T. Kassem Bustamente, H. Duque Caro.

JAMES (D.E.), 1984. — Quantitative models for crustal contamination in the Central and the Northern Andes. In Andean Magmatism (Eds : Harmon and Barreiro) : 124-138. Shiva Pub. Cheshire, UK.

JAMES (D.E.) and MURCIA (L.A.), 1984. — Crustal contamination in Northern Andean volcanics. *J. Geol. Soc. London*, 141 : 823-831.

JARAMILLO (J.M.), 1980. — Petrology and geochemistry of the Nevado del Ruiz volcano, Colombia, Northern Andes. *Ph. D. thesis. Univ. Houston. Houston Tex.*, 167 p.

KELLOG (J.N.), OGUJIOFLOR (I.J.), KANSAKAR (D.R.), 1985. — Panama and North Andean block tectonics (abstr.). *Eos*, 66, 46 : 1088.

LEAKE (B.E.), 1978. — Nomenclature of amphiboles. *Amer. Mineral.*, 63 : 1023-1052.

LINDSLEY (D.H.), 1983. — Pyroxene thermometry. *Amer. Mineral.*, 68 : 477-493.

LOPEZ-ESCOBAR (L.), 1984. — Petrology of volcanic rocks of the Southern Andes. In « Andean Magmatism » (Eds : R.S. Harmon and B.A. Barreiro) : 47-71. Shiva Pub. Cheshire, UK.

LOWE (D.R.), WILLIAMS (S.N.), LEIGH (H.), CONNOR (C.B.), GEMMELL (J.B.), STOIBER (R E), 1986. — Lahars initiated by the 13 November 1985 eruption of Nevado del Ruiz, Colombia. *Nature*, 324 : 51-53.

MAGONTHIER (M.C.), 1984. — Les ignimbrites de la Sierra Madre Occidental et de la province uranifère de la Sierra Peña Blanca, Mexique. *Thèse Doct. Sci. Nat. Univ. P.M. Curie, Paris*, 322 p.

MARRINER (G.E.), MILLWARD (D.), 1984. — The petrology and geochemistry of cretaceous to recent volcanism in Colombia : The magmatic history of an accretionary plate margin. *J. Geol. Soc. London*, 141 : 473-486.

McCOURT (J.J.), ASPDEN (J.A.), BROOK (M.), 1984. — New geological and geochronological data from the Colombian Andes : Continental growth by multiple accretion. *J. Geol. Soc. London*, 141 : 473-486.

MÉGARD (F.) — Cordilleran Andes and marginal Andes : A review of Andean geology North of the Arica elbow (18°S). *In* « Circum Pacific orogenic belts and the evolution of the Pacific ocean basin (Eds : J.W.H. Monger and J. Francheteau). *Amer. Geophys Union. Geodyn. ser* (In press)

MURCIA (A.), 1982. — El vulcanismo plio-cuaternario de Colombia depositos piroclasticos asociados y mediciones isotopicas de $^{87}$ Sr / $^{86}$ Sr, $^{143}$ Nd / $^{144}$ Nd y $\delta$ $^{18}$ O en lavas de los volcanes Galeras, Purace y Nevado del Ruiz *Publ. Geol. Esp., Ingeominas,* 10 1-17. Bogota.

NARANJO (J.L.), SIGURDSSON (H.), CAREY (S.N.), FRITZ (W.), 1986. — Eruption of the Nevado del Ruiz volcano, Colombia, on 13 November 1985 : tephra fall and lahars. *Science.* 233 : 961-963.

NAKAMURA (N.), 1974. — Determination of REE, Ba, Fe, Mg, Na and ordinary chondrites *Geochim. Cosmochim. Acta,* 38 : 757-775

O'CALLAGHAN (L.J.), FRANCIS (P.W.), 1986. — Volcanological and petrological evolution of San Pedro volcano, Provincia el Poa. North Chile. *J. Geol. Soc. London,* 143 : 275-286.

OLIVER (R.A.), KERR (S.A.), 1981 — ILL Experimental Report 03 12.21.

PEARCE (J.A.), 1983. — Role of the sub-continental lithosphere in magma genesis at active continental margin. *In* : « Continental Basalt and Mantle Xenoliths » (Eds : Hawkesworth and Norry) : 230-250, Shiva Pub Cheshire, UK.

PECCERILLO (A.) and TAYLOR (S.R.), 1976. — Geochemistry of Eocene calc-alkaline volcanic rocks from the Kastamonu area, Northern Turkey. *Contrib Mineral. Petrol.,* 58 : 63-81.

POWELL (R.), POWELL (M.), 1977. — Geothermometry and oxygen barometry using coexisting iron-titanium oxides a reappraisal. *Mineral. Mag.,* 41 257-263

ROBINSON (P.), SCHUMACHER (J.C.), SPEAR (F.S.), 1982. — Phase relations of metamorphic amphiboles : natural occurrence and theory. Formulation of electron probe analyses. *In* « Reviews in Mineralogy 8B Amphiboles : Petrology and Experimental Phase Relations » (Ed D.R. Veblen and P.H. Ribb) : 6-9 Mineral Society of America Bookcrafters, Inc Chelsea Michigan 48118 USA.

RYMER (H.), BROWN (G.C.). 1984 — Periodic gravity changes at Poas Volcano. Costa Rica. *Nature.* 311 : 242-245.

STOUT (J.H.), 1972. — Phase petrology and mineral chemistry of coexisting amphibole from Telemark, Norway. *J. Petrol.,* 13 99-146

THORPE (R.S.), FRANCIS (P.W.), O'CALLAGHAN (L.), 1984. — Relative roles of source composition, fractional crystallisation and crustal contamination in the petrogenesis of Andean volcanic rocks. *Phil Trans. R. Soc. Lond.,* A 310 : 675-692.

THORPE (R.S.), LOCKE (C.A.), BROWN (G.C.), FRANCIS (P.W.), RANDAL (M.). 1981. — Magma chamber below Poàs volcano, Costa Rica *J. Geol. Soc. London,* 138 : 367-373.

THORPE (R.S.), POTTS (P.J.), FRANCIS (P.W.), 1976. — Rare Earth data and petrogenesis of andesites from the North Chilean Andes *Contrib. Mineral Petrol.,* 54 65-75.

THOURET (J.C.), 1984. — Observations géomorphologiques préliminaires sur quelques reliefs volcaniques des Andes Centrales de Colombie. Géomorphologie, exemples Sud-américains. *Trav. et Doc. CEGET-CNRS.* 52 : 96-128.

THOURET (J.C.), GOURGAUD (A.), CALVACHE (M.L.), *(in press).* — The 13 November 1985 eruption at Nevado del Ruiz : a preliminary analysis of eruptive mechanisms, morphological and glaciological changes on and around the ice-cape and petrology of products. *Boletin geológico. Publicaciones Geológicas Especiales, Ingeominas.*

THOURET (J.C.), JANDA (R.J.) PIERSON (T.C.), CALVACHE (M.L.), CENDRERO (A.), 1987. — L'éruption du 13 novembre 1985 au Nevado del Ruiz (Cordillère Centrale, Colombie) : interactions entre le dynamisme éruptif, la fusion glaciaire et la genèse d'écoulements volcano-glaciaires. *C. R. Acad. Sci. Paris,* 305, 2 : 505-509.

THOURET (J.C.), MURCIA (A.L.), SALINAS (R.E.), VATIN-PÉRIGNON (N.), 1985a. — Cronoestratigraphia mediante dataciones K/Ar y $^{14}$ C de los volcanes compuestos del complejo Ruiz-Tolima y aspectos volcano-estructurales del Nevado del Ruiz (Cordillera Central, Colombia). *Sexto Congreso Latinoamericano de Geologia.* Medellin, Colombia : 387-454.

THOURET (J.C.), VATIN-PÉRIGNON (N.), CANTAGREL (J.M.), SALINAS (R.), MURCIA (A.), 1985b. — Apports des premières datations K-Ar et $^{14}$C à la chronostratigraphie des volcans composites et aspects volcano-structuraux du Nevado del Ruiz (Cordillère Centrale des Andes de Colombie). *Bull. Assoc. Géogr. Franç.,* 2 128-134.

THOURET (J.C.), VATIN-PÉRIGNON (N.), CANTAGREL (J.M.), SALINAS R.), MURCIA (A.), 1985c. — Le Nevado del Ruiz (Cordillère Centrale des Andes de Colombie) stratigraphie, structures et dynamisme d'un appareil volcanique andésitique, composé et polygénique *Rev. géol. et géogr. phys.,* 26 (5) 257-271.

VATIN-PÉRIGNON (N.), GOEMANS (P.), OLIVER (R.A.), THOURET (J.C.), SALINAS (R.E.), MURCIA (A.L.), 1987. — Magmatic evolution of the calc-alkaline Nevado del Ruiz volcano, Central Cordillera, Colombia. Part I : Geochemistry. ORSTOM Bondy (France). Séminaire « *Andes Centrales* » : 41-42.

VATIN-PÉRIGNON (N.), OLIVER (R.A.), GOEMANS (P.), 1987. — Petrogeochemistry and evolution of the Nevado del Ruiz volcano, Central Cordillera, Colombia (abstr.) *Terra Cognita.* 7 : 2-3, 280.

VATIN-PÉRIGNON (N.), VIVIER (G.), VITTOZ (P.), OLIVER (R.A.), THOURET (J.C.), SALINAS (E.), A. MURCIA (L.), 1985. — REE concentrations in some volcanic rocks from a cross-section through the Central Cordillera, Colombia . Cauca Basin, Nevado del Ruiz, Casabianca Formation *Comunicaciones.* 35 : 243-247.

VATIN-PÉRIGNON (N.), VIVIER (G.), VITTOZ (P.), THOURET (J.C.), OLIVER (R.A.), SALINAS (E.), A. MURCIA (L.), 1986. — Petrochemistry of Late Pleistocene to Holocene volcanic products of the Nevado del Ruiz, Central Cordillera, Colombia (abstr.). *Eos,* 16 405-406.

WILLIAMS (S.N.), STOIBER (R.E.), GARCIA (P.N.), LONDONO (C.A.), GEMMELL (J.B.), LOWE (D.R.), CONNOR (C.B.), 1986. — Eruption of the Nevado del Ruiz Volcano, Colombia, on 13 November 1985 Gas Flux and Fluid Geochemistry. *Science,* 233 : 964-967.

WOOD (B.J.), BANNO (S.), 1973. — Garnet-orthopyroxene and orthopyroxene-clinopyroxene relationships in simple and complex systems. *Contrib. Mineral Petrol.,* 42 : 109-124.